Transcritical and Hopf Bifurcations in Lumped Parameter LMFBR Dynamical Systems

by

V. BALAJI

ET
90
1
AL
RA

TH
NET/1998/M
B 182

to the

NUCLEAR ENGINEERING AND TECHNOLOGY PROGRAMME

INDIAN INSTITUTE OF TECHNOLOGY KANPUR

JULY 1998

Transcritical and Hopf Bifurcations in Lumped Parameter LMFBR Dynamical Systems

A Thesis Submitted
in Partial Fulfilment of the Requirements
for the the Degree of

MASTER OF TECHNOLOGY

by
V. BALAJI

to the

NUCLEAR ENGINEERING AND TECHNOLOGY PROGRAMME
INDIAN INSTITUTE OF TECHNOLOGY KANPUR

JULY 1998

Acc. No. A 126236

NETP-1988-M-BAL-TRA

A126236

I.I.T. Kanpur.
Submitted on 23.7.98

Certificate

It is certified that work reported in the thesis entitled *Transcritical and Hopf Bifurcations in Lumped Parameter LMFBR Dynamical Systems* by V.BALAJI, has been carried out under my supervision and that this work has not been submitted elsewhere for a degree.

PROFFESSOR M. S. KALRA

Department of Mechanical engineering

and

Nuclear Engineering and Technology Programme

INDIAN INSTITUTE OF TECHNOLOGY KANPUR

July 1998

Acknowledgements

I would like to express my deep sense of gratitude to my guide Dr. M. S. Kalra for introducing me to the theory of bifurcation, for suggesting this problem, and patiently guiding me throughout this work.

I dutifully acknowledge the help and advice of Prof. Prabhat Munshi who acted as a friend and counsellor throughout my stay at IITK. My heartiest thanks to him.

I express my deep sense of gratitude to my parents for their love, affection and encouragements. I take this as an opportunity to express my love and affection to my brother. His adorable patience and encouragement will remain with me forever.

My colleaques Surash Babu, Satyaprakash and Ram Manohar deserve special mention for their support and understanding which helped me in many ways. I strongly appreciate their willingness to help whenever asked for. Words are not sufficient to express my thankfulness to all my friends who made my stay at Hall-IV indeed memorable.

It is a pleasure to acknowledge the care and affection extended to me by the NET family members. My heartiest thanks to all of them.

Abstract

Lumped paramter LMFBR dynamical systems based on effective lifetime and prompt-jump approximations, and one and six groups of delayed neutrons are analyzed for transcritical and Hopf bifurcations. Besides the core, a simple model of secondary heat exchanger, as well as suitable models for control reactivity, are also included. Both the proportional and the differential controllers are considered.

Data for analysis is derived for physical parameter values available for a large number of LMFBRs. The analysis shows that none of the LMFBRs considered is likely to experience Hopf bifurcation. It is also found that the transcritical bifurcation occurs only when higher-order feedback effects are present. But even then the bifurcation occurs for a positive value of the coolant temperature reactivity feedback. These conclusions remain true even when we combine the dimensionless parameters in the worst manner within certain stipulated ranges.

Inclusion of control reactivity is shown to make bifurcations in the lumped parameter LMFBR models further unlikely for all negative gains.

Contents

Acknowledgement i

Abstract ii

Contents iii

List of figures v

List of tables vii

Nomenclature ix

1 Introduction 1

1.1 Motivation....1

1.2 Objectives....2

1.3 Review of Literature....2

1.4 Outline of the Present Work....4

1.5 A Brief Description of LMFBR....4

1.6 Reactivity Effects in LMFBRs....5

2 Lumped Parameter LMFBR Dynamical Systems 9

2.1 Neutron Kinetics 9
2.2 Power Balances 10
2.3 Steady State Relations 12
2.4 Linear Reactivity Feedback 12
2.5 Dimensionless Equations 13
2.6 Six Groups of Delayed Neutron Precursors 16
2.7 Simpler Dynamical Models 18
2.8 Higher-Order Feedback 20
2.9 Control Reactivity Feedback 21
2.10 Input Data 22

3 Analytical and Computational Techniques **26**

3.1 Normal Forms at Bifurcation Points 33
3.2 Location of Bifurcation Points 42
3.3 Calculation of Center Manifolds 34
3.4 Calculation of Trajectories 38
3.5 Poincare Sections and Charateristic Multipliers 39

4 Numerical Results, Discussions, and Conclusions **40**

4.1 Stability at Full Power Operation 40
4.2 Critical Parameter Values 42
4.3 Simultaneous Variation of Parameters 46
4.4 Trajectories, Bifurcation Diagrams and Phase Portraits 48
4.5 Critical Values for the Control Reactivity 50
4.6 Conclusions and Observations 52

References **65**

Appendix A **69**

List of Figures

1. A schematic diagram of a two-temperature LMFBR model with and without secondary heat exchanger.....6

2a A schematic diagram of static bifurcation.....28

2b A schematic diagram of Hopf bifurcation.....28

3a Schematic diagram of saddle node bifurcation.....29

3b Schematic diagram of pitch fork bifurcation.....29

3c Schematic diagram of transcritical bifurcation.....29

4a A schematic diagram of a normal (supercritical) bifurcation.....30

4b A schematic diagram of a subcritical (inverse) bifurcation.....30

4c A schematic diagram of coexistence of stable and unstable solutions in a subcritical Hopf bifurcation.....31

5. Time variation of dimensionless power $\wp$ subsequent to transcritical bifurcation in a LMFBR core (worst case) 54

6. Time variation of dimensionless coolant temperature $\Im_c$ subsequent to transcritical bifurcation in an LMFBR core (worst case).....55

7. Effect of secondary heat exchanger and groups of delayed neutrons on time variation of dimensionless fuel temperature $\Im_f$ subsequent to transcritical temperature in a LMFBR core.....56

8. Bifurcation diagram (with and without secondary heat exchanger) for transcritical bifurcation in the worst case LMFBR.....57

9. Bifurcation diagram (with and without secondary heat exchanger) for transcritical bifurcation in the worst case LMFBR.....58

10. Bifurcation diagram (with and without secondary heat exchanger) for transcritical bifurcation in the worst case LMFBR.....59

11. Behavior of Dimensionless Power (neutron flux) versus time in LMFBR core (worst case) subsequent to Hopf bifurcation using one group of delayed neutrons ($\varepsilon = 0.01$).....60

12. Phase portrait of limit cycles in LMFBR models on $\wp - \Im_f$ plane (worst case) subsequent to Hopf bifurcation ($\varepsilon = 0.01$).....61

13. Phase portrait of limit cycles in LMFBR models on $\Im_f - \Im_c$ plane (worst case) subsequent to Hopf bifurcation ($\varepsilon = 0.01$).....62

14. Behavior of Dimensionless Power (neutron flux) versus time in LMFBR core (worst case) subsequent to Hopf bifurcation using six groups of delayed neutrons ($\varepsilon = 0.01$).....63

15. Effect of secondary heat exchanger on the limit cycles in the worst case LMFBR subsequent to Hopf bifurcation ($\varepsilon = 0.01$).....64.

List of Tables

1. Input data for LMFBRs.....23

2. Input data and dimensionless parameters.....24

3. Input data for six groups of delayed neutrons.....24

4. Dimensionless parameters for LMFBRs based on data given in Table 1.....25.

5. Reactor Period for operation at full power for the Reference LMFBR (SUPER PHENIX).....41

6. Reactor Periods at full power operation for the LMFBRs shown in Table 1 (using six groups of delayed neutrons).....42

7. Critical Values of the coolant temperature coefficient of reactivity ( ) for static and dynamic bifurcations for the Reference LMFBR core (SUPER PHENIX).....44

8. Effect of secondary heat exchanger (HE) on the critical values for static bifurcation for the reference LMFBR (SUPER PHENIX).....44

9. Effect of secondary heat exchanger (HE) on the critical values for dynamic bifurcation for the reference LMFBR (SUPER PHENIX).....45

10. Critical Values of coolant temperature coefficient of reactivity ( ) for Static and Dynamic Bifurcations for the LMFBRs listed in Table 1.....45

11. Ranges of Parameter Ratios allowed for the worst case LMFBR.....47

12. Values of the Parameter Ratios for the worst case LMFBR for static and dynamic bifurcations within the limits given in Table 11.....47

13. The stability parameter a and the characteristic (Floquet) multiplier for the LMFBR core limit cycle (worst case).....50

14. Critical Values of the coolant temperature coefficient of reactivity ( ) for different values of K_p and t_p for the reference reactor (SUPER PHENIX) using six groups of delayed neutrons.....51

15. Critical Values of the control parameter K_c for Hopf bifurcation for reference LMFBR (SUPER PHENIX).....52

Nomenclature

A list of symbols is given below. Some symbols which are specific to a section, and whose meaning may be different in different sections, are not included. Standard mathematical symbols also do not appear in the list.

Roman

a_c	$\dfrac{\alpha_c(T_{co}-T_d)}{\beta}$, dimensionless
a_C	$\alpha_C(T_{co}-T_d)^2/\beta$, dimensionless
a_f	$\dfrac{\alpha_f(T_{fo}-T_d)}{\beta}$, dimensionless
a_F	$\alpha_F(T_{fo}-T_d)^2/\beta$, dimensionless
$a(0)$	normal form parameter $a(\varepsilon)$ at $\varepsilon = 0$
b	$\dfrac{\lambda\Lambda}{\beta}$, a nondimensionless parameter
b(0)	a normal form parameter $b(\varepsilon)$ at $\varepsilon = 0$
c	C_f / C_c

C_c	heat capacity of coolant in reactor core, JK^{-1}
C_f	heat capacity of fuel elements in core, JK^{-1}
C_m	heat capacity of the moderator in the calandria, JK^{-1}
C_s	effective heat capacity of the secondary side, JK^{-1}
$\subset$	$(C-C_o) / C_o$
N, N(t)	number of neutrons
p	$\dfrac{\Lambda P_0}{\beta C_f (T_{f0} - T_{c0})}$
P, P(t)	reactor power, W
$\wp$	$\dfrac{P - P_o}{P_o} = \dfrac{N - N_o}{N_o}$
r	$\dfrac{\Lambda P_o}{C_s \beta (T_{co} - T_{so})}$
t	time, s
T	time-period or characteristic time (in specified units or dimensionless)
T_c, T_c (t)	average coolant temperature, K
T_f, T_f (t)	average fuel temperature, K
$\Im_c$	$\dfrac{T_c - T_{co}}{T_{co} - T_i}$
$\Im_f$	$\dfrac{T_f - T_{fo}}{T_{fo} - T_i}$
$\Im_s$	$\dfrac{T_s - T_{so}}{T_{co} - T_{so}}$

U, U(η)	Jacobian matrix of the vector field at **X**=0
V (X,η)	vector field
W(X,η)	nonlinear part of the vector field
X, X(τ)	state vector at time τ

Greek

α_c	coolant temperature coefficient of reactivity, K^{-1}
α_f	fuel temperature coefficient of reactivity, K^{-1}
α_C	second order coolant temperature coefficient of reactivity, K^{-2}
α_F	second order fuel temperature coefficient of reactivity, K^{-2}
β	one group delayed neutron fraction
η	a set of dimensionless parameters
λ	one-group decay constant for delayed neutron precursors, s^{-1}
Λ	neutron reproduction or generation time, s
θ	$\dfrac{T_{co} - T_d}{T_{fo} - T_d}$
ρ	reactivity, dimensionless
ρ_{fb}	feedback reactivity
ρ_c	control reactivity
ρ_X	reactivity feedback due to xenon-135
τ	βt / Λ , dimensionless time
ϕ	flux of thermal neutrons, $m^{-2}\ s^{-1}$
Φ, Φ(t)	fundamental or state transition matrix

Miscellaneous

$	ρ / β

Subscripts

R	a reference value
o	a steady state value

Superscripts

*	a critical value

Chapter 1

Introduction

1.1 Motivation

Mathematical formulations of physical problems often result in differential equations that are nonlinear. Nonlinear systems are used to describe a great variety of phenomena, in the physical and engineering sciences as well as in the life and social sciences. Nuclear reactors are no exceptions and are being increasingly analyzed as nonlinear systems. In particular certain concepts in bifurcation theory, chaos and fractals are likely to become more and more relevant to the safe operation of nuclear reactors. Bifurcations occur where the solutions of the nonlinear systems change in their qualitative character, as the parameters are changed. The theory of bifurcation, therefore, concerns all nonlinear systems and hence has a great variety of applications.

It is well known that even with linear reactivity feedback effects, the dynamic models of the nuclear reactors are nonlinear. Nonlinearities in the reactor dynamical systems arise in general, due to strong interactions between the neutronics, thermal hydraulics and fission product poisoning. (Fission product poisoning is of less importance in LMFBRs

which are the subject of the present study.) Under conditions involving large departures from the intended steady state, an intrinsically nonlinear system such as a nuclear reactor, may exhibit a response that has no counterpart in the linear world.

No general method is available for solving nonlinear differential equations and. unlike linear systems; few nonlinear systems possess closed form solutions. The emergence of computers as new tools for theoretical physics and engineering studies have favored the development of nonlinear dynamics. Numerical simulations have made the richness of nonlinear models accessible to the intuition of the physicists and engineers.

At the present time it appears, however, that the techniques of nonlinear systems research have not been as fully and widely applied in the nuclear energy field as in other branches of science and engineering. The present work tries to bring out some aspects of nonlinear dynamics (local transcritical and Hopf bifurcations) in some LMFBR models.

1.2 Objectives

The overall objective of the present work is to study the phenomenological lumped parameter models of LMFBRs in order to understand the role of reactor core nonlinearities arising due to fuel and coolant temperature reactivity feedbacks. A simple model of the secondary heat exchanger (HE) and control reactivity feedback is also included. Emphasis will be on identifying the parameter ranges over which the local bifurcation phenomenon may take place.

1.3 Review of Literature

The literature in the area of LMFBR dynamical systems is reviewed here. A two temperature feedback model for the PWR is discussed by Manmohan in his doctoral

thesis (1996). Based on the above work a two temperature feedback model for the LMFBR is presented in this work.

The mathematical and physical importance of the nonlinear form of reactor kinetics equations, when the effect of temperature is included, was pointed out by Chernick (1951). Robinson (1954, 1955) extended the treatment of Chernick (1951) in regard to concept of reactor stability and included the effect of delayed neutrons. The concepts of orbital, secular and asymptotic stability are examined in the phase plane representation and techniques are pointed out whereby the effect of the delayed neutrons on reactor kinetics may be taken into consideration. Hsu (1968), Kastenberg (1968), and Hsu and Sha (1969) considered the stability problem for spatially dependent nonlinear reactor systems and pointed out that in a practical reactor the delayed neutrons must be included and more than one feedback should be considered. Enginol (1985) has analyzed asymptotic stability of nuclear reactors with arbitrary nonlinear feedback. Adebiyi and Harms(1989, 1990) examine some aspects of linear and nonlinear nuclear reactor kinetics by general topological methods. Dorning(1989) provides a general discussion of strange atrractors in the context of nuclear reactors. Yang and Cho (1992) present expansion methods for finding nonlinear stability domains of nuclear reactor models.

A model for simulating the transients in LMFBR is discussed by Agrawal and Yang(1977). Lewins (1987) discusses various methods for the control of nuclear reactors. The models for the secondary heat exchanger are also discussed. Edwards and Lee (1990) have described a new control concept, state feedback assisted classical control for nuclear reactors and power plants. An improved reactivity table model for LMFBR dynamics is described by Stacey (1972). Some of the physical, technical, safety, and material problems of fast reactors are presented by Karl Wirtz (1973).

. Hummel and Okrent (1970) have discussed the reactivity coefficients and their effects in LMFBRs. Data and methods for calculating reactivity coefficients are introduced. The significance of reactivity coefficients for the operation and safety of LMFBRs is well discussed. A detailed discussion of transcritical and Hopf Bifurcations is provided in Guckenheimer and Holmes (1983).

1.4 Outline of the present work

A brief description of LMFBRs and reactivity effects of temperature is presented in section 1.5 later in this chapter. Chapter 2 consists of formulations of lumped parameter models for the LMFBR dynamical systems for the core, secondary heat exchanger and control systems based on one or Six groups of delayed neutrons. Models based on effective lifetime and prompt-jump approximations are also presented. All the governing equations are presented in a dimensionless form.

In Chapter 3, the phenomenon of transcritical and Hopf bifurcation in the LMFBR dynamical systems is investigated. Center manifold is calculated for the transcritical and Hopf bifurcations . Various numerical methods involved in calculating the bifurcation points in different models are also discussed.

The behavior of LMFBR dynamical systems in the close vicinity of the bifurcation point is studied by numerical simulations. The results of these are presented in Chapter 4. A summary of work done and the possible extension of the present work, are also presented in Chapter 4.

1.5 A Brief Description Of LMFBRs.

If the main source of fission is the capture of fast neutrons directly by the fuel without the neutrons having suffered appreciable energy losses, the system is called a fast neutronic system. The fuel consists of two parts, a core, (highly) enriched in $U^{235}/Pu^{239}/U^{233}$, and a U^{238}/Th232 breeder blanket. The reactor is sodium cooled and operates at temperatures which do not approach boiling. Such reactors are called Liquid Metal Fast Breeder Reactors.

The use of liquid sodium, Na-23, as coolant ensures that there is little neutron moderation in the fast reactor. The element sodium melts at 371K, boils at 1156K, and has excellent

heat transfer properties. With such a high melting point, pipes containing sodium must be heated electrically and thermally insulated to prevent freezing. The coolant becomes radioactive by neutron absorption, producing the 15h halflife Na-24. Great care must be taken to prevent contact between sodium and water or air, which would result in a serious fire, accompanied by the spread of radioactivity. To avoid such an event, an intermediate heat exchanger is employed, in which heat is transferred from radioactive sodium to nonradioactive sodium.

Some of the major differences between thermal reactors and fast breeder reactors, from a dynamical viewpoint are:

(1) The prompt lifetime of the fast reactors is a few orders of magnitude smaller than that of thermal reactors, being of the order of 10^{-7} s.

(2) The temperature coefficients of reactivity are generally smaller than those in the thermal reactors and there is no fast acting, large dominant temperature coefficient which overrides all the others.

(3) The delayed neutron fraction β for fast fission of U^{235} is about fifty percent smaller than that for the thermal fission of U^{235}.

(4) The total excess reactivity in a fast reactor is small. The excess reactivity is small because fission-product poisoning is small, and the amount of reactivity needed for temperature override is small.

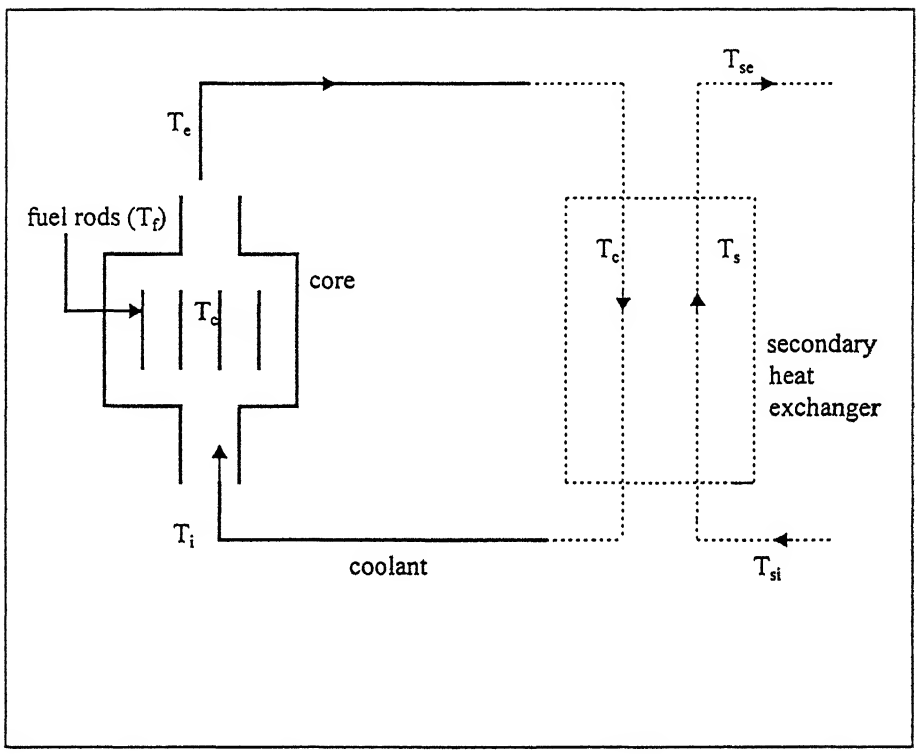

Figure 1: A schematic diagram of a two-temperature LMFBR model with secondary heat exchanger

1.6 Reactivity effects in LMFBRs

In a LMFBR three effects on reactivity require special attention which are:

i)Sodium void effect,

ii)Doppler effect, and

iii)other temperature effects.

Although the reactivity effect due to fission product poisoning of xenon and samarium plays an important role in thermal reactors, we can safely neglect their effect in a fast reactor such as an LMFBR, as the absorption cross-section of xenon and samarium is very low for fast neutrons. We will now briefly explain the reactivity effects due to sodium voiding , Doppler broadening of fission and capture resonances, and temperature.

Sodium void effect occurs due to loss of some or all sodium from a fast reactor. Reactivity temperature coefficients in a fast reactor can be both prompt and delayed. The prompt coefficient arises mainly from the Doppler effect in the fuel, but in some cases neutron leakage can be important. The delayed coefficient results from a number of factors associated with the expansion of the liquid sodium coolant when the temperature is increased.

The reactivity effect resulting from Doppler broadening of fission and capture resonances arises from a varying competition among fission, capture, and leakage processes. The Doppler effect (by Doppler effect we mean the change in multiplication factor associated with an arbitrary change in fuel temperature) in large, fast power reactors occurs almost entirely below 25 kev, because cross section variations with temperature become very small at higher energies . Since leakage in such reactors is

relatively small at low energies, their Doppler effect can be regarded as resulting from a varying competition between fission and capture. This phenomenon causes a difference in fission-source neutrons produced per neutron absorption at low energies.

The change in this ratio (neutrons produced per neutron absorbed) for some energy below which practically all the Doppler effect occurs (perhaps 25 kev) multiplied by the fraction of total fission-source neutrons slowing down below that energy is approximately equal to the Doppler effect. The importance of the Doppler effect lies in its provision, for reactors with a high concentration of fertile material, of a prompt, negative reactivity effect from fuel heating.

Chapter 2

Lumped Parameter LMFBR Dynamical Systems

2.1 Neutron Kinetics

The neutron kinetics equations with one group of delayed neutrons can be written as (Lewins 1978, Hetrick 1965) :

$$\frac{dN}{dt} = \frac{\rho-\beta}{\Lambda}\mathrm{N} + \lambda\,\mathrm{C}, \quad \text{and} \tag{2.1}$$

$$\frac{dC}{dt} = \frac{\beta}{\Lambda}\mathrm{N} - \lambda\,\mathrm{C}, \tag{2.2}$$

where

N = N(t) is the number of neutrons or average neutron density in the reactor,

C = C(t) is the number of delayed neutron precursors or average delayed neutron precursor density,

t = time (s),

Λ = neutron reproduction or generation time (s),

β = delayed neutron fraction (dimensionless),

λ = decay constant for delayed neutron precursors (s^{-1}), and

ρ = reactivity or fractional excess multiplication constant (dimensionless).

2.2 Power Balances

The two temperature feedback model is based on two power balances: one for the energy contained in the fuel elements of the reactor core, and another for the energy stored in the coolant within the core volume. Although a small fraction of energy released in the fission process is directly deposited in the coolant, this is ignored.

The power balance for the *fuel elements* is given by

$$C_f \frac{dT_f}{dt} = P - H_f(T_f - T_c), \tag{2.3}$$

where

T_f = $T_f(t)$ is the average fuel temperature(K),

T_c = $T_c(t) = \frac{T_e + T_i}{2}$ is the mean coolant temperature(K),

P = P(t) is the reactor power(W),

C_f = heat capacity of the fuel elements in the reactor core(J K^{-1}),

and

H_f = fuel to coolant heat transfer constant(W K^{-1}).

The power balance for the *coolant* in the reactor core is given by

$$C_c \frac{dT_c}{dt} = H_f(T_f - T_c) - 2\dot{m}c_c(T_c - T_i), \tag{2.4}$$

where

C_c = heat capacity of the coolant in the reactor core(J K^{-1}),

T_i = coolant inlet temperature(K),

$\dot{m}_c$ = mass flow rate of coolant through the core (kg s^{-1}),

c_c = specific heat of the coolant (J kg^{-1} K^{-1}).

The power balance for the *secondary heat exchanger* is given by

$$C_s \frac{dT_s}{dt} = H_s(T_c - T_s) - 2\dot{m}_s c_s(T_s - T_{si}) \tag{2.5}$$

where

C_s = heat capacity for the secondary side(J K^{-1}),

T_{si} = secondary side inlet temperature (K),

$T_s = \frac{T_{se} + T_{si}}{2}$ is the average temperature corresponding to the secondary side (K),

$\dot{m}_s$ = Secondary side flow rate(kg s^{-1})

H_s = primary to secondary side heat transfer constant (WK^{-1})

2.3 Steady State Relations

The steady state operating values of the state variables in Eqs. 2.1-2.5 will be denoted by N_o, C_o, T_{fo}, T_{so} and T_{co}, respectively, and the steady state value of the reactivity is taken as ρ_o. By equating Eqs 2.1-2.5 to zero, we obtain

$$\rho_o = 0, \qquad C_0 = \frac{\beta}{\Lambda} N_o$$

$$H_f = \frac{P_o}{(T_{fo} - T_{co})}, \qquad 2\dot{m}c_c = \frac{P_o}{(T_{co} - T_{io})}$$

$$H_s = \frac{P_o}{(T_{co} - T_{so})} \qquad 2\dot{m}_s C_s = \frac{P_o}{(T_{so} - T_{si})}, \tag{2.6}$$

T_{io} is the steady state value of the reactor inlet temperature, T_i. It is assumed to be constant if secondary heat exchanger is not included in the model. Otherwise, T_{si}, the inlet temperature to the secondary heat exchanger is considered constant.

2.4 Linear reactivity Feedback

The reactivity ρ appearing in Eq. 2.1 can, in general, be written as

$$\rho = \rho_o + \rho_e(t) + \rho_c + \rho_{fb} \tag{2.7}$$

As seen above, if there is no external source of neutrons in the reactor, as is the case considered throughout the present work, $\rho_o = 0$. For the autonomous systems we treat in this work, $\rho_e(t) = 0$. The control reactivity ρ_c is considered separately in section 2.10 Further, the dynamical systems developed in this section are based on linear reactivity feedback which for the two temperature LMFBR model can be written as

$$\rho = \rho_{fb} = \alpha_f (T_f - T_{fo}) + \alpha_c (T_c - T_{co}), \tag{2.8}$$

where

α_f = fuel temperature coefficient of reactivity(K^{-1}), and

α_c = coolant temperature coefficient of reactivity(K^{-1}).

Higher order feedback terms are considered later in section 2.8.

It is the substitution of Eq. 2.8 in Eq. 2.1 which is one source of nonlinearity in the fission reactor dynamical systems. It leads to the product terms of N(t) or P(t) with both $T_f(t)$ and $T_c(t)$. Instead of presenting the resulting equations, we first choose suitable nondimensional forms of the dependent state variables and the independent time variable.

2.5 Dimensionless Equations

In order to obtain the previous equations in a dimensionless form we choose the following translation and scaling of the state variables and time:

$$\wp = \frac{P - P_o}{P_o} \equiv \frac{N - N_o}{N_o}, \qquad \subset = \frac{C - C_o}{C_o}$$

$$\Im_f = \frac{T_f - T_{fo}}{T_{fo} - T_d}, \qquad \Im_c = \frac{T_c - T_{co}}{T_{co} - T_d},$$

$$\tau =. \frac{\beta}{\Lambda} t \text{ , and} \qquad \Im_s = \frac{T_s - T_{so}}{T_{co} - T_{so}}, \tag{2.9}$$

where $T_d = T_{io}$ if the secondary heat exchanger is excluded from the model, and $T_d = T_{so}$, if the secondary heat exchanger is included.

The translations of the state variables in the above equations shift the operating or equilibrium point to the origin. This is essential for the analysis presented in later chapters. The normalizations used could be chosen differently, but the above choice puts the dynamical system in the simplest form. Substitution of Eqs. 2.8 and 2.9 into Eqs. 2.1-2.5 and using Eqs. 2.6 where needed leads to the following dimensionless system:

$$\frac{d\wp}{d\tau} = -\wp + \subset + a_f\,\Im_f + a_c\,\Im_c + a_f\,\wp\Im_f + a_c\,\wp\Im_c, \tag{2.10}$$

$$\frac{d\subset}{d\tau} = b(\wp - \subset), \tag{2.11}$$

$$\frac{d\Im_f}{d\tau} = p(1-\theta)\wp - p\Im_f + p\vartheta\Im_c. \tag{2.12}$$

If the secondary heat exchanger is excluded from the model, we have for the dimensionless coolant temperature $\Im_c$:

$$\frac{d\Im_c}{d\tau} = \frac{pc}{\theta}(\Im_f - \Im_c). \tag{2.13}$$

If the secondary heat exchanger is included in the model then we have the following equations for $\Im_c$ and $\Im_s$:

$$\frac{d\Im_c}{d\tau} = \frac{pc}{\theta}\left(\Im_f - \Im_c + (1-\theta)\Im_s\right), \tag{2.13a}$$

$$\frac{d\Im_s}{d\tau} = r\left(\Im_c - (1+\Theta)\Im_s\right), \tag{2.14}$$

where

$$a_f = \frac{\alpha_f(T_{f0} - T_d)}{\beta}, \qquad a_c = \frac{\alpha_c(T_{c0} - T_d)}{\beta},$$

$$b = \frac{\lambda\Lambda}{\beta}, \qquad p = \frac{\Lambda P_0}{\beta C_f (T_{f0} - T_{c0})},$$

$$\theta = \frac{T_{co} - T_d}{T_{fo} - T_d}, \qquad c = \frac{C_f}{C_c},$$

$$r = \frac{\Lambda P_o}{\beta C_s (T_{so} - T_{si})}, \qquad \Theta = \frac{T_{co} - T_{so}}{T_{so} - T_{si}} \tag{2.15}$$

It can been seen that the original system of two temperature feedback model has been transformed to a dimensionless system with six or eight nondimensional parameters, depending on whether the secondary heat exchanger is excluded or included in the model. The parameters a_f and a_c can been interpreted as the dimensionless measures of temperature coefficients of reactivity. The parameter p may be understood to measure the steady state power Po of the reactor. The other parameters are viewed as simple dimensionless combinations of input quantities involving times, temperatures and heat capacities.

Equations 2.10-2.14 can been written in the form of a state equation:

$$\begin{aligned} \dot{\mathbf{X}} &= \mathbf{V}(\mathbf{X},\eta) \\ &= \mathbf{U}(\eta)\mathbf{X} + \mathbf{W}(\mathbf{X},\eta) \end{aligned} \tag{2.16}$$

where the overdot denotes the derivative with respect to the dimensionless time τ, **X** is the state vector, η is the set of dimensionless parameters (Eqs. 2.15), and $\mathbf{V}(\mathbf{X},\eta)$ is the vector field whose linear part is $\mathbf{U}(\eta)\mathbf{X}$ and the non linear part is $\mathbf{W}(\mathbf{X},\eta)$, i.e.,

$$\mathbf{X} = \begin{bmatrix} X_1 \\ X_2 \\ X_3 \\ X_4 \\ X_5 \end{bmatrix} = \begin{bmatrix} \wp \\ \subset \\ \Im_f \\ \Im_c \\ \Im_s \end{bmatrix}, \quad \mathbf{W}(\mathbf{X},\eta) = \begin{bmatrix} a_f X_1 + a_c X_4 \\ 0 \\ 0 \\ 0 \\ 0 \end{bmatrix}$$

$$\mathbf{U}(\eta) = \mathbf{D_x V}(\mathbf{X_o},\eta) = \begin{bmatrix} -1 & 1 & a_f & a_c & 0 \\ b & -b & 0 & 0 & 0 \\ p(1-\theta) & -p & p\theta & 0 & 0 \\ 0 & 0 & d & -d & 0 \\ 0 & 0 & 0 & r & -r(1+\Theta) \end{bmatrix} \tag{2.17}$$

$$\eta = \{a_f \quad a_c \quad b \quad c \quad p \quad r \quad \Theta\}$$

$$\begin{bmatrix} \dot{\wp} \\ \dot{\subset} \\ \dot{\Im}_f \\ \dot{\Im}_c \\ \dot{\Im}_s \end{bmatrix} = \begin{bmatrix} -1 & 1 & a_f & a_c & 0 \\ b & -b & 0 & 0 & 0 \\ p(1-\theta) & -p & p\theta & 0 & 0 \\ 0 & 0 & d & -d & 0 \\ 0 & 0 & 0 & r & -r(1+\Theta) \end{bmatrix} \begin{bmatrix} \wp \\ \subset \\ \Im_f \\ \Im_c \\ \Im_s \end{bmatrix}$$

2.6 Six Group of Delayed Neutron Precursors

Six groups appear to be optimum for an accurate representation of delayed neutron precursors. For the calculation of the critical value of a parameter at which a bifurcation

may take place, it is therefore desirable to use six groups of delayed neutrons. This is achieved by replacing Eq. 2.11 by six differential equations governing the population of different delayed neutron precursors:

$$\frac{d\subset_i}{d\tau} = b_i(\wp - \subset_i), \qquad i=1,\ldots,6,$$

where

$$\subset_i = \frac{\subset_i - \subset_{i0}}{\subset_{i0}},$$

$\subset_i$ = population of the precursor group i,

$\subset_{i0}$ = steady state population of the precursor group i,

$$b_i = \frac{\lambda_i \Lambda}{\beta}$$

$$\beta = \sum_{i=1}^{6} \beta_i ,$$

β_i = delayed neutron fraction for the ith precursor group,

λ_i = decay constant of the ith precursor group,

and other variables or constants are as defined earlier in this chapter. The term $\subset$ in Eqs 2.10 is replaced by:

$$\subset = \sum_{i=1}^{6} a_i \subset_i$$

where $a_i = \frac{\beta_i}{\beta}$ is the relative yield for the precursor group i. For the purpose of parameter variations in six group models, instead of treating each b_i as a variable parameter, we write

$$b_i = \left(\frac{\lambda_i}{\lambda}\right) b, \text{ and } \lambda = \frac{1}{\sum_{i=1}^{6} \frac{a_i}{\lambda_i}},$$

where b has been previously defined (Eqs 2.15) and is treated as a possibly variable parameter as in one-group models.

2.7 Simpler Dynamical Models

In the dynamical models presented in the previous section, the delayed neutrons have been treated using a one or six precursor groups. One precursor group is often convenient and satisfactory. Further simplification is afforded by the effective lifetime and the prompt jump approximations. Below these models are briefly described and the governing equations are presented in the dimensionless form as used in the present work.

Effective Lifetime Model

The effective lifetime Λ' of neutrons may be defined as (Hetrick, 1971; Lewins, 1978):

$$\Lambda' = \Lambda + \frac{\beta}{\lambda} \approx \frac{\beta}{\lambda} \tag{2.18}$$

If, in the preceding equations, Λ is replaced by Λ', and the state variables as well as the equations corresponding to the delayed neutron precursor are dropped, we obtain the lumped parameter dynamic equations based on the effective lifetime of neutrons. This model is sometimes easier to analyze but is applicable only when the reactivity and the rate of change reactivity are small :

$$\frac{1}{\lambda}\left|\frac{d\rho}{dt}\right| << |\rho| \;<<\; \beta, \tag{2.19}$$

or, in terms of the dimensionless variables used in this work,

$$|\$| << 1, \text{ and } \quad \left|\frac{d\$}{d\tau}\right| << b|\$|$$

where $\$ = \frac{\rho}{\beta}$ and b is defined earlier in this chapter.

Prompt-Jump Approximation

The prompt-jump approximation or, as it is sometimes called, the zero-lifetime approximation, is described in detail by Hetrick (1971). Formally, an expansion of the neutron population or density in powers of the small parameter Λ is attempted, the procedure being analogous to the method of singular perturbations. If this approximation is used, the point-reactor kinetics Eqs. 2.1 and 2.2 are replaced by the following single equation :

$$\frac{dN}{dt} \approx \frac{\lambda\rho + \frac{d\rho}{dt}}{\beta - \rho} N \tag{2.20}$$

In Eq. 2.20 the reactivity ρ must be substituted through Eq. 2.8, in terms of the other variables. This makes Eq. 2.20 for the neutron population nonlinear, as is the case in other models. The criterion for the validity of prompt-jump approximation is (Hetrick, 1971):

$$\frac{1}{N}\left|\frac{dN}{dt}\right| << \frac{\beta - \rho}{\Lambda} \tag{2.21}$$

It should be noted that the criterion (2.21) can only be satisfied if $\rho < \beta$, i.e., $\$ < 1$. In terms of the dimensionless variables defined earlier, the prompt-jump approximation can be written as

$$\dot{\wp} \approx \frac{(1+\wp)(\$ + \dot{b}\mathbb{S})}{1-\$}, \tag{2.22}$$

which is applicable if the following condition, equivalent to (Eq. 2.21), is satisfied:

$$\frac{\left|\dot{\wp}\right|}{(1+\wp)(1-\$)} << 1. \tag{2.23}$$

where the overdot denotes derivatives with respect to the dimensionless time τ defined earlier.

2.8 Higher-Order Feedback

Higher-order feedback terms do not play a significant role in Hopf bifurcation (Manmohan, 1996). However, as will be seen later in this work, they play a crucial role in the transcritical bifurcation. We describe below the higher-order feedback reactivity as follows:

$$\rho = \rho_{fb} = \rho_{fb}^{(1)} + \rho_{fb}^{(2)} + \ldots\ldots, \tag{2.24}$$

with

$$\rho_{fb}^{(1)} = \alpha_f (T_f - T_{fo}) + \alpha_c (T_c - T_{co}) \ , \tag{2.25}$$

$$\rho_{fb}^{(2)} = \alpha_F (T_f - T_{fo})^2 + \alpha_C (T_c - T_{co})^2 , \tag{2.26}$$

where α_F and α_C denote the second order reactivity feedback coefficients for the fuel and the coolant , respectively, and the other symbols are as used earlier in this chapter. It is to be noted that the units of α_F and α_C are K^{-2}, while those of the linear feedback coefficients, α_f and α_c are K^{-1}. Introducing Eqs. 2.24-2.26 in Eqs 2.7 and 2.1, and making use of the nondimensional variables and parameters already defined, we can write the first equation in reactor kinetics as follows:

$$\frac{d\wp}{d\tau} = -\wp + \subset + a_f \Im_f + a_c \Im_c + a_f \wp \Im_f + a_c \wp \Im_c + a_F \Im_f^{\ 2} + a_C \Im_c^{\ 2} + a_F \wp \Im_f^{\ 2} + a_C \wp \Im_c^{\ 2} \tag{2.27}$$

where

$$a_F = \alpha_F (T_{fo} - T_d)^2 / \beta,$$

$$a_C = \alpha_C (T_{co} - T_d)^2 / \beta,$$

and all other parameters are as defined earlier.

2.9 Control Reactivity Feedback

In the present work we consider a simple control model based on proportional and differential controllers. The control may be based on the fractional change in reactor power and / or a suitably defined fractional change in reactor coolant temperature. Thus the control reactivity ρ_c can be written as

$$\rho_c = K_p(\wp + t_p \frac{d\wp}{dt}) + K_c(\Im_c + t_c \frac{d\Im_c}{dt}), \tag{2.28}$$

where

K_p = (negative) constant (gain) proportional to the fractional change in power represented by the dimensionless power $\wp$

K_c = (negative) constant (gain) proportional to the fractional change in coolant temperature represented by the dimensionless coolant temperature $\Im_c$, and

t_p, t_c = time constants associated with the differential controller based on the rate of change of power or coolant temperature, respectively.

Inclusion of control reactivity changes only the first equation in the original system presented earlier. If the differential controller is included then the resulting equation is suitably recast by transferring the derivative terms on the LHS, or substituting their values in terms of state variable from other equations.

The resulting equation governing the dimensionless power is given bel

$$(1-k_p\tau_p)\left[1-\frac{k_p\tau_p}{1-k_p\tau_p}\wp\right]\dot{\wp}=(-1+k_p)\wp+\subset+(a_f+k_c\tau_c d)\Im_f+(a_c+k_c-k_c\tau_c d)\Im_c$$

$$+\ldots\ldots\ldots\ldots\ldots\ldots,$$

where

$$k_p=\frac{K_p}{\beta}\ ,\quad k_c=\frac{K_c}{\beta}\ ,\quad \tau_p=\frac{t_p\beta}{\Lambda}\ ,\text{and}\quad \tau_c=\frac{t_c\beta}{\Lambda}$$

Here only the linear terms on the RHS have been retained. As we will see later, analysis based on these linear terms show that bifurcation (static or dynamic) takes place for very large (negative) values of K_p or K_c, which are unlikely to occur in practice. As a result the higher-order terms on the RHS are not required in the present work.

2.10 Input Data

The set of input values that we need to know for each reactor model to carry out the analysis and computations have been arrived at in the preceding sections of this chapter. The input data are evaluated from the reactor data available from Power Reactors, (1983)and World Nuclear Industry Handbook (1994). Data of eleven different LMFBRs is given in Table 1. For reactors of different designs, or under different operating conditions, the input data can be widely different.

Table 1: Input data † for LMFBRs

Reactor	P_o	C_f	C_c	T_{fo}	T_{co}	T_{io}
	MWt	MJK^{-1}	MJK^{-1}	K	K	K
SUPER-PHENIX	3000	5.355	8.21	1583	743.0	668
BELOYARSK-3	1470	2.72	1.538	1628	736.5	650
BELOYARSK-4	2100	2.72	1.538	1628	736.5	650
DFR	60	0.057	0.09	1283	754.0	673
EBR-2	62.5	0.078	0.07	868	694.5	644
JOYO	100	0.08	0.186	1848	708.0	643
KARLSRUHE	58	0.232	0.226	1865.5	715.5	633
MANGYSHLASKI	1000	0.39	1.497	1373	628.0	553
MONJU	714	1.888	1.635	1785.5	736.0	670
PHENIX	563	1.376	0.773	1773	753.0	673
FBTR	40	0.047	0.03	1473	718.5	653

† The meaning of each symbol is given in the Nomenclature and explained in the text.

A sample calculation for the values of C_f and C_c is given in Appendix A. Table 2 gives the reference values for one group reactor-kinetics parameters as well as the corresponding dimensionless parameters. Table 3 gives the six group of delayed neutron data. The dimensionless parameters are given in Table 4 are calculated based on data given in Table 1. The value of the parameter r in Table 4 is based on,

$$C_s = 0.02 \text{ Full-power-second (FPS).}$$

Table 2: Input data † and dimensionless parameters for one-group reactor-kinetics

Input Values		Dimensionless Parameters	
Symbol	Value	Symbol	Value
β	0.0035	b	2×10^{-6}
λ	$0.07\ s^{-1}$	a_f	-1.045
Λ	$10^{-7}\ s^{-1}$	a_c	-0.128
α_f	$-4 \times 10^{-6}\ K^{-1}$	r ‡	0.000029
α_c	$-6 \times 10^{-6}\ K^{-1}$		

† The meaning of each symbol is given in the Nomenclature and explained in the text.

‡ This value of r is calculated on the basis of : $C_s = 0.02$ FPS,
$T_{so} = T_{co}-50$, $T_{si} = T_{io}-50$.

Table 3: Input data for six groups of delayed neutrons

Group i	Relative Yield a_i	Decay Constant $\lambda_i\ (s^{-1})$
1	0.038	0.0127
2	0.213	0.0317
3	0.188	0.115
4	0.407	0.311
5	0.128	1.40
6	0.026	3.87

Table 4.: Dimensionless parameters ‡ for LMFBRs based on data given in table1

Reactor	p	c	θ	Θ †
SUPER-PHENIX	0.000019	0.652	0.081	0.667
BELOYARSK-3	0.000017	1.768	0.088	0.578
BELOYARSK-4	0.000025	1.768	0.088	0.578
DFR	0.000057	0.633	0.132	0.617
EBR-2	0.000132	1.114	0.225	0.990
JOYO	0.000031	0.43	0.053	0.769
KARLSRUHE	0.000006	1.026	0.066	0.606
MANGYSHLASKI	0.000098	0.26	0.091	0.667
MONJU	0.000010	1.154	0.059	0.757
PHENIX	0.000011	1.78	0.072	0.625
FBTR	0.000032	1.566	0.079	0.763

† These values are calculated on the basis of : $C_s = 0.02$FPS,
$T_{so} = T_{co}-50$, $T_{si} = T_{io}-50$

‡ The meaning of each symbol is given in the Nomenclature and explained in the text.

Chapter 3

Analytical and Computational Techniques

Several analytical and computational techniques are needed to locate the bifurcation points and to investigate the behavior of the dynamical system in the vicinity of these points. These have been discussed in detail by Wiggins (1989) , and Parker and Chua (1989) . The techniques required for the analysis of Hopf bifurcation are also developed by Manmohan (1996). A *bifurcation* describes a qualitative change in the dynamics when the parameters in the system are varied. The values of the parameters where this change takes place are called bifurcation values or critical values. Knowledge of bifurcation is absolutely essential for the complete understanding of the system. Below we summarize the methods used in the present work for the study of both the static and Hopf bifurcations in LMFBR systems.

3.1 Normal Forms at Bifurcation Points

A static bifurcation occurs when an eigenvalue crosses the imaginary axis through the origin. On the other hand if a pair of complex conjugate eigenvalues cross the imaginary

axis transversally a Hopf bifurcation occurs This is illustrated in Figures 2a and 2b. In both the cases three different situations may arise. For Hopf bifurcation this is illustrated in Figures 3a-3c, and for the static bifurcation this is illustrated in Figures 4a-4c.

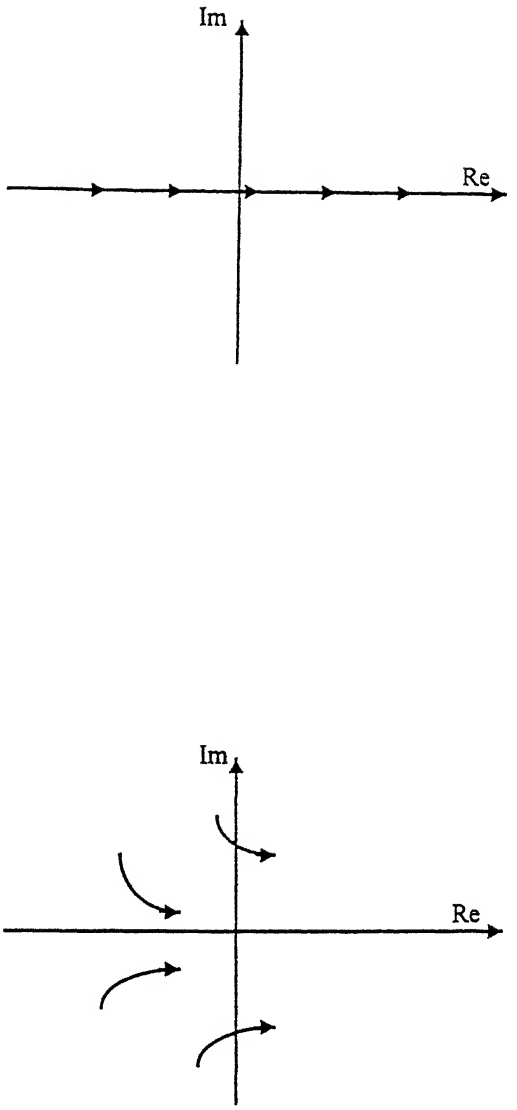

Figure 2 : A schematic diagram of (a) static bifurcation (b) hopf bifurcation

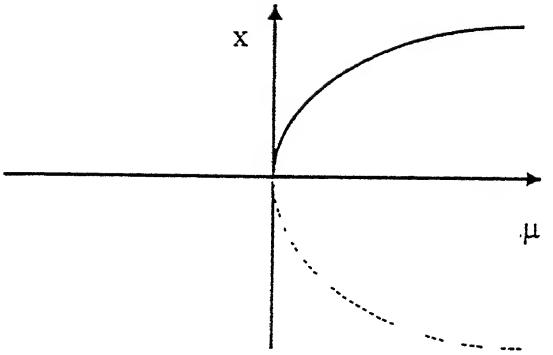

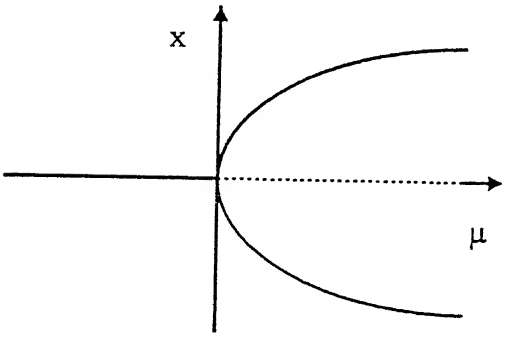

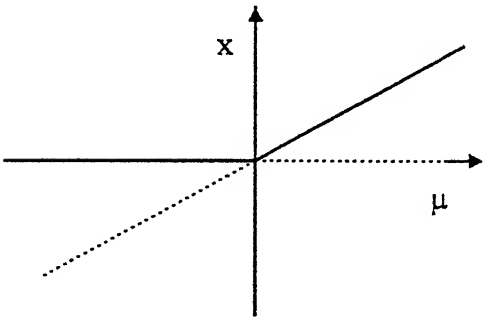

Figure 3: Schematic diagrams of (a) saddle-node (b) pitchfork and (c) transcritical bifurcations

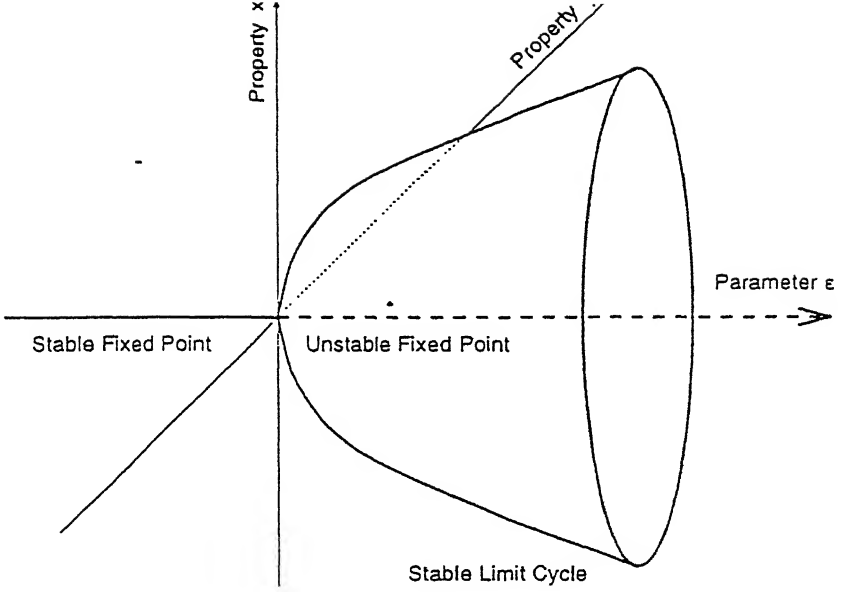

Figure 4: (a) A schematic diagram of a normal (Supercritical) Hopf bifurcation

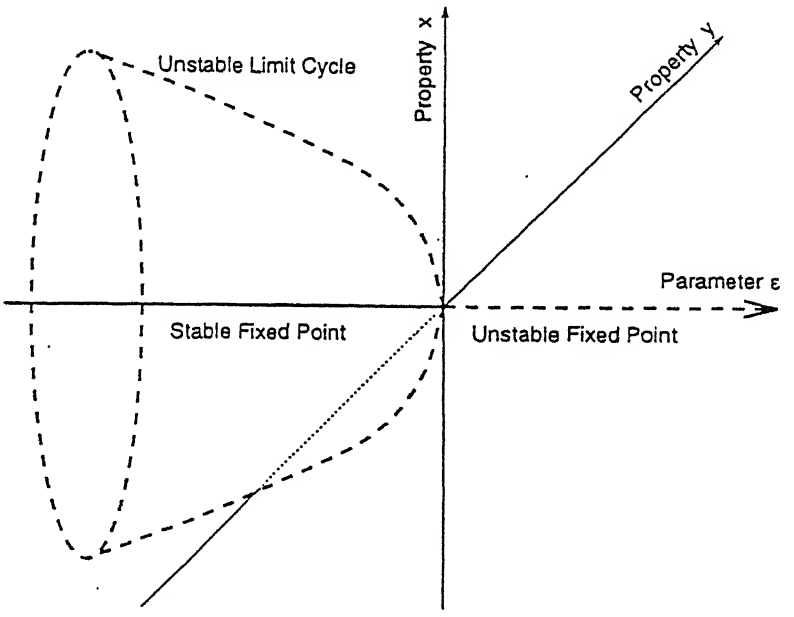

Figure 4 : (b) A schematic diagram of a subcritical (inverse) Hopf bifurcation

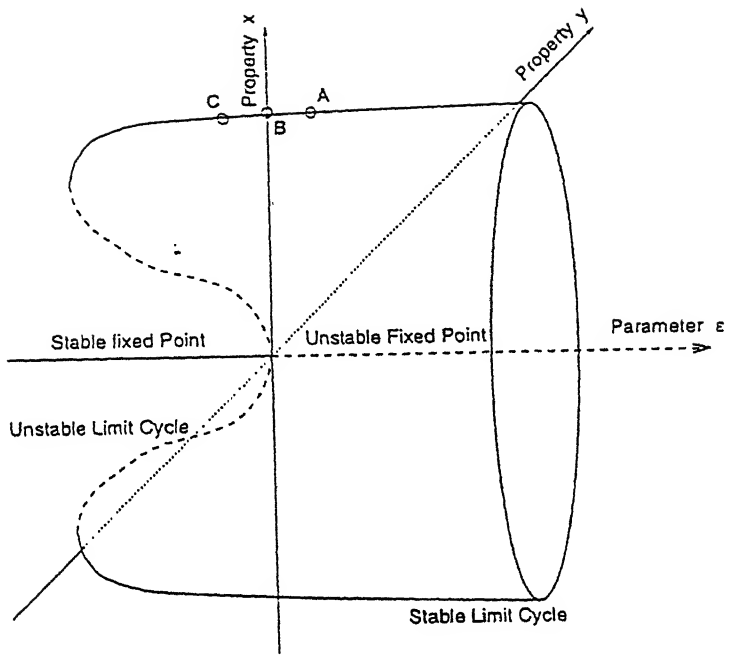

Figure 4 : (c) A schematic diagram of Coexistence of unstable and stable solutions in a subcritical Hopf bifurcation

Poincare Normal Form

A systematic way to ascertain the effect of the nonlinear terms is to reduce the dynamical system to a two dimensional center manifold, which is then transformed to the Poincare normal form. The proof that this can be done may be found in Wiggins (1989). Here, we state the main results related to the Poincare normal form and introduce some notations used in the calculations. The Poincare normal form in the Cartesian coordinates, x_1 and x_2 for Hopf bifurcation, can be written as

$$\dot{x}_1 = \alpha(\varepsilon)x_1 - \omega(\varepsilon)x_2 + [a(\varepsilon)x_1 - b(\varepsilon)x_2](x_1^2 + x_2^2) + \ldots\ldots \qquad (3.1)$$

$$\dot{x}_2 = \omega(\varepsilon)x_1 + \alpha(\varepsilon)x_2 + [b(\varepsilon)x_1 + a(\varepsilon)x_2](x_1^2 + x_2^2) + \ldots\ldots \qquad (3.2)$$

where the normal form parameters $a(\varepsilon)$ and $b(\varepsilon)$ are defined for all sufficiently small ε. The parameter $a(0)$, called the *stability parameter*, determines the stability of bifurcating periodic solutions (Wiggins 1989):

(i) The case $a(0) < 0$: The bifurcation is normal (supercritical).

(ii) The case $a(0) > 0$: The bifurcation is inverse (subcritical).

Remark : A simple proof of the above statements, facilitated by considering Poincare normal form in polar coordinates, may be found in Wiggins (1989).

We now give below the normal forms for the three kinds of static bifurcations namely saddle-node, pitchfork, and transcritical bifurcation

- The normal form for the saddle-node bifurcation is given by,

  $\dot{x} = \varepsilon \pm x^2$

- The normal form for the pitchfork bifurcation is given by,

$$\dot{x} = \varepsilon x \mp x^3$$

- The normal form for transcritical bifurcation is given by,

$$\dot{x} = \varepsilon x \mp x^2$$

In the above equations ε is the variable parameter. Let $\mu \in \eta$, and μ^* be the value of μ at which the bifurcation occurs. Then ε is defined as

$$\varepsilon = \frac{\mu - \mu^*}{\mu^*}$$

3.2 Location of Bifurcation Points

Several techniques have been discussed in the literature for the location of the bifurcation point (Kubicek and Marek, 1983). In general the algorithms used are iterative in nature and make use of the Newton-Raphson method to find the critical value of the parameter. The critical value μ^* of $\mu \in \eta$ is located by solving the equation

$$\alpha(\mu) = 0 \tag{3.3}$$

where $\alpha(\mu)$ denotes the real part of a complex conjugate pair of eigenvalues of the matrix $U(\eta)$, evaluated at the steady state / equilibrium (operating) point.

The QR Method

The eigenvalues of the matrix $U(\eta)$ for a given set of parameter values are calculated using the QR algorithm. The Jacobian matrices associated with the dynamical systems studied in the present work are, in general, nonsymmetric. Since a nonsymmetric matrix may not be balanced, it is first replaced by a balanced matrix with identical eigenvalues (Press, et al., 1993). This reduces the sensitivity of the eigenvalues to rounding errors during numerical computations. The matrix is then reduced to a simpler Hessenberg form

and the eigenvalues are calculated by using the standard QR algorithm applicable to real Hessenberg matrices.

Newton-Raphson Iteration

The Newton-Raphson algorithm is used to find the solution of Eq 3.3. Since the success of a locally convergent scheme depends critically on having a good first guess for the solution, it is desirable to use a globally convergent method which guarantees some progress towards the solution at each iteration. Perhaps the best strategy is to bracket the root and then refine it by a combination of the Newton-Raphson and the bisection methods. This keeps the root within the brackets while taking advantage of the rapid local convergence of the Newton-Raphson method. We have mostly used this kind of approach in this work.

3.3 Calculation of Center Manifolds

Center manifolds play an important role in the organization of system orbits in the phase space. This is due to the fact that these are invariant under the flow generated by the dynamical system. The center manifold plays a particularly crucial role in the study of a bifurcation. It isolates the complicated asymptotic behavior by locating the invariant manifold tangent to the center eigenspace, i.e., the subspace spanned by the eigenvectors corresponding to the eigenvalues on the imaginary axis.

Hopf Bifurcation

Calculation of center manifolds and normal forms requires considerable amount of algebra, [referred to as *Horrendous* by Wiggins (1989)] particularly for the 2-

dimensional Hopf bifurcation. These algebraic aspects are investigated in detail by Manmohan (1996) and in the present work we used the same computer program to determine the stability parameter, a(0), occurring in the Poincare normal form. We first consider the parameter independent case and let $\mathbf{U}=\mathbf{U}(\eta^*)$ and $\mathbf{W}(\mathbf{X}) = \mathbf{W}(\mathbf{X},\eta^*)$ to simplify the notation.

In order to calculate the center manifold of the dynamical system

$$\dot{\mathbf{X}} = \mathbf{U}\mathbf{X} + \mathbf{W}(\mathbf{X}) \tag{3.4}$$

$$\text{let} \quad \mathbf{X} = \mathbf{S}\mathbf{Y}$$

where S is the matrix whose columns are the eigenvectors of U. Thus we have

$$\dot{\mathbf{Y}} = (\mathbf{S}^{-1}\mathbf{U}\mathbf{S})\mathbf{Y} + \mathbf{S}^{-1}\mathbf{W}(\mathbf{S}\mathbf{Y}) \tag{3.5}$$

$$= \Lambda\mathbf{Y} + \mathbf{S}^{-1}\mathbf{W}(\mathbf{S}\mathbf{Y}) \tag{3.6}$$

Equation 3.2 can be separated into two parts :

$$\begin{aligned} \dot{u} &= \mathbf{A}u + \mathbf{F}(\mathbf{u},\mathbf{v}) \\ \dot{v} &= \mathbf{B}v + \mathbf{G}(\mathbf{u},\mathbf{v}) \end{aligned} \tag{3.7}$$

where

$$\mathbf{A} = \begin{bmatrix} 0 & \omega_o \\ -\omega_o & 0 \end{bmatrix}, \qquad \mathbf{Y} = \begin{bmatrix} \mathbf{u} \\ \mathbf{v} \end{bmatrix}$$

Then the introduction of another nonlinear transformation

$$\mathbf{v} = \mathbf{h}(\mathbf{u}) \tag{3.8}$$

followed by elimination of quadratic terms in the resulting equations is required to obtain the Poincare normal form. For details reference should be made to Wiggins(1989), Manmohan(1996).

Static Bifurcation

The transformations required for the calculation of center manifold/normal form for static bifurcation are similar to those for the Hopf bifurcation, but considerably simpler due to

one-dimensional nature of the manifold. We illustrate it using one-group LMFBR model., The center manifold **u**, (Eq. 3.7) is one-dimensional and we can write it as

$$\dot{u} = F(u,v)$$

$$\text{let } v_i = h_i(u), \qquad i=1,2,....,n-1.$$

$$= b_i u^2$$

As shown in Wiggins(1989), each $h_i(u)$ must satisfy

$$\frac{dh_i}{du} F(u,h(u)) - \Lambda_i h_i - G_i(u,h(u)) = 0, \qquad i = 1,2,...n-1. \tag{3.9}$$

where

$$\Lambda = \begin{bmatrix} 0 & . & . & . & . & 0 \\ . & \Lambda_1 & . & . & . & . \\ . & . & \Lambda_2 & . & . & . \\ . & . & . & . & . & . \\ . & . & . & . & . & . \\ 0 & . & . & . & . & \Lambda_{n-1} \end{bmatrix} \text{ is a diagonal matrix.}$$

It is straightforward to see that if only linear feedback is used solution of Eq 3.9 yields,

$$b_i = 0, \quad i=1,...,n-1.$$

Thus, the center manifold / normal form has no quadratic terms. If all b_i's are zero, and the original nonlinear terms in **W(X)** do not contain cubic terms (as is the case with linear feedback), the center manifold or normal form also do not contain any cubic terms.

Thus with linear feedback, all the three types of static bifurcation are ruled out, and the behavior of the nonlinear system remains divergent as would have been the case in the linear system. This is in conformity with the fact that, with linear feedback, no additional equilibrium (fixed) point originates from the operating point, i.e., (0,0,...0).

If higher-order reactivity feedback effects are present, then, as shown in Section 2.8, these introduce additional quadratic and cubic terms in the system (Eq. 2.27) , Due to the

cubic terms, an additional equilibrium solution / fixed point of interest emerges. It is easy to see that without the secondary heat exchanger, this fixed point is given by (using one group of delayed neutrons)

$$\wp = \subset = \Im_f = \Im_c = -\frac{a_f + a_c}{a_F + a_C},$$

and with the secondary heat exchanger, this is given by

$$\wp = \subset = 0, \qquad \Im_f = \frac{\theta + \Theta}{1 + \Theta}\Im_c, \qquad \Im_s = \frac{\Im_c}{1 + \Theta},$$

where

$$\Im_c = \frac{(-ka + A) \pm SQRT((ka + A)^2 - 4kaA)}{2kA} \tag{3.10}$$

where

SQRT denotes the square root.

$$k = \frac{\Theta}{1 + \Theta},$$

$$a = \frac{\theta + \Theta}{1 + \Theta} a_f + a_c,$$

$$A = \left(\frac{\theta + \Theta}{1 + \Theta}\right)^2 a_F + a_C$$

In Eq 3.10 only one of the solution bifurcates from the origin, indicating transcritical bifurcation, and excluding the possibility of saddle node and pitchfork bifurcations. (The saddle node bifurcation is also excluded by the fact that the original equilibrium point, (0,0,...0), does not remain stable beyond the bifurcation point). The fact that at the bifurcation point, exchange of stability occurs, is brought out in the diagrams shown in Chapter 4.

As can been seen from Eq 2.27, the higher-order feedback effects introduce into the system not only the cubic terms, but additional quadratic terms. As a result, the quadratic terms in the normal form can no longer be zero and thus the normal form will correspond to that of transcritical bifurcation.

3.4 Calculation of Trajectories

Calculation of trajectories by numerical integration is perhaps the most important and expensive task in the simulation of a dynamical system. It is also a prerequisite for the application of geometric tools or mathematical constructs such as Poincare sections, phase portraits and the calculation of characteristic multipliers or Lyapunov exponents.

Over the years, a large number of algorithms have been developed to approximate the behavior of a continuos-time system on a digital computer. A proper choice of the method and a careful application play a crucial role in the computational accuracy and efficiency. Among the available methods, the major practical choices are the single step methods, the multistep predictor-corrector methods, and the Bulirsch-Stoer extrapolation methods. The most popular among the single step methods are the Runge-Kutta methods. Both explicit and implicit implementations of the methods mentioned above are available in literature. The choice depends on the stiffness of the system to be integrated. In the present work an implicit implementation of Bulirsch-Stoer method given by Press, etal (1993) is used.

3.5 Poincare sections and Characteristic Multipliers

In order to simplify the phase space diagrams of a dynamical system of order n, one introduces an (n-1) dimensional surface of sections in the phase space and. instead of studying a complete trajectory, one monitors only the points of its intersection with this surface. A set of points of intersection of the trajectory with a hypersurface, as the trajectory crosses the surface from one side to the other, is referred to as *Poincare section.* Mapping an intersection point onto the subsequent intersection point is referred to as the *Poincare (return) map.*

The stability of periodic solutions or closed orbits is determined by the characteristic (Floquet) multipliers or roots. These can be regarded as a generalization of the eigenvalues at an equilibrium point. According to standard Floquet theory, the stability of a periodic orbit is determined by the eigenvalues of the monodromy matrix $\Phi(T)$ (also referred to as Floquet transition matrix), which is simply defined as the value of the fundamental matrix at the time period T, with the initial value as the unit matrix I (Kubicek and Marek 1983). If these eigenvalues lie within the unit circle in the complex plane, the periodic solution is stable. It is well known that one of the eigenvalues of $\Phi(T)$ is always unity (Husseyin, 1986; Parker and Chua 1989). Thus a periodic orbit can never be asymptotically stable. The remaining eigen values of $\Phi(T)$ determine the *orbital* stability and are called the characteristic multipliers.

In the present work, we confirm the existence of limit cycles (whenever these occur) using Poincare sections, and calculate the characteristic multipliers using a method based on Poincare return maps (Manmohan 1996). The numerical results for both the transcritical and Hopf bifurcations are reported and discussed in the next chapter.

Chapter 4

Numerical Results, Discussions, and Conclusions

Numerical simulations are required to confirm the predictions of the theoretical considerations given in Chapter 3. Furthermore, the theory is valid only in an arbitrarily small neighborhood of the bifurcation points. As one moves away from this neighborhood, numerical calculations are often the only means of obtaining information about the nature of solutions. In this chapter, we present the numerical results for the lumped parameter LMFBR dynamical systems developed in Chapter 2.

4.1 Stability at Full Power Operation

Before proceeding to calculate the critical values of parameters for which bifurcations may occur and simulating the behavior subsequent to bifurcation, it is desirable to confirm the stability of the systems considered at their normal operating values. In reactor dynamical systems this is indicated by *reactor period*, T_p, or the e-folding time (Glasstone, 1994)

$$T_p = P / \frac{dP}{dt} \equiv \frac{1}{\omega_o}$$

where ω_o is the real part of the eigenvalue closest to the imaginary axis. The eigenvalues are calculated for the Jacobian matrix. U (Eq. 2.17) , evaluated at the normal operating point. A negative reactor period indicates stability at the point under consideration.

Table 5 shows the (negative) reactor periods for the reference LMFBR, SUPER PHENIX, using five dynamical models presented in Chapter 2. It can be seen that for all the models, both with and without secondary heat exchanger, reactor stability is indicated at the normal fullpower steady state operation. This is also the case for other reactors studied. This is indicated in Table 6 using six groups of delayed neutrons.

Table 5: Reactor Period for operation at full power for the Reference LMFBR (SUPER PHENIX)

Reactor Model	Negative Reactor Period (s)	
	Without HE	With HE
No delayed neutrons	1.31×10^2	1.22×10^2
Effective life-time model	1.02×10^1	0.8×10^1
Prompt-jump approximation	2.57×10^1	0.45×10^1
One group of delayed neutrons	2.57×10^1	2.42×10^1
Six groups of delayed neutrons	9.15×10^1	9.11×10^1

Table 6: Reactor periods at full power operation for the LMFBRs shown in Table 1 (using six groups of delayed neutrons)

Reactor	Negative Reactor Periods (s)	
	Without HE	With HE
SUPER PHENIX	9.11×10^1	9.15×10^1
BELOYARSK-3	9.10×10^1	9.12×10^1
BELOYARSK-4	9.10×10^1	9.12×10^1
DFR	9.23×10^1	9.32×10^1
EBR-2	9.83×10^1	10.5×10^1
JOYO	9.04×10^1	9.08×10^1
KARLSRUHE	9.02×10^1	9.05×10^1
MANGYSHLASKI	9.14×10^1	9.20×10^1
MONJU	9.06×10^1	9.10×10^1
PHENIX	9.06×10^1	9.10×10^1
FBTR	9.15×10^1	9.12×10^1

4.2 Critical Parameter Values

For the purpose of bifurcation studies, we have treated the coolant temperature coefficient of reactivity, α_c , as the variable parameter, keeping all other parameters fixed. (A simultaneous variation of all parameters with a view to find the worst combination is presented later.) The critical values α_c^* for the static and dynamic bifurcations for the reference reactor SUPER PHENIX core are presented in Table 7 using

- No delayed neutrons

- Effective lifetime model
- Prompt-jump approximation
- One group of delayed neutrons
- Six groups of delayed neutrons

It can been seen that the critical values for Hopf bifurcation differ considerably on the model employed. In fact the, prompt-jump approximation does not yield any critical values for the Hopf bifurcation. For this reason, unless otherwise indicated, we have used one-group and six-group models only.

The effect of secondary heat exchanger on the critical values, α_c^*, is brought out in Table 8 and 9, for the transcritical and Hopf bifurcation, respectively, using one and six groups of delayed neutrons. While the effect of the number of groups of delayed neutrons is relatively small, the effect of the secondary heat exchanger on the critical value is considerable.

Table 10 shows the critical values for other reactors using six groups of delayed neutrons and including the secondary heat exchanger in the model. It can be seen from Tables 7 to 10, that the static (transcritical) bifurcation occurs for *positive* value of the coolant (sodium) temperature coefficient of reactivity (α_c), while the dynamic (Hopf) bifurcation occurs for negative values of the same. For most LMFBRs, the actual values of α_c is likely to be negative, and of the order of 10^{-5} K^{-1}. While the order of magnitude of α_c^* (transcritical bifurcation) is close to it, it is opposite in sign. On the other hand, while the sign of α_c^* for Hopf bifurcation is negative, its magnitude is extremely high. Thus Hopf bifurcation in any of the reactors studied is completely ruled out. A static bifurcation may occur if the coolant (sodium) temperature coefficient of reactivity becomes positive.

Table 7: Critical values of the coolant temperature coefficient of reactivity (α_c) for Static and Dynamic bifurcations for the Reference LMFBR core (SUPER PHENIX)

Reactor Model	Critical value, α_c^* K^{-1}	
	Static	Dynamic
No delayed neutrons	4.88×10^{-5}	-6.14×10^{-6}
Effective life time model	4.88×10^{-5}	-3.99×10^{-3}
Prompt jump approximation	4.88×10^{-5}	---------
One group of delayed neutrons	4.88×10^{-5}	-3.29
Six groups of delayed neutrons	4.88×10^{-5}	-3.13

Table 8: Effect of Secondary Heat Exchanger on the critical values for Static Bifurcation for the Reference LMFBR (SUPER PHENIX)

Reactor Model	Critical Value, α_c^* (K^{-1})	
	Core	Core + HE
One group of delayed neutrons	4.88×10^{-5}	3.09×10^{-5}
Six groups of delayed neutrons	4.88×10^{-5}	3.09×10^{-5}

Table 9: Effect of Secondary Heat Exchanger on the critical values for Dynamic Bifurcation for the Reference LMFBR (SUPER PHENIX)

Reactor Model	Critical Value, α_c^* (K^{-1})	
	Core	Core + HE
One group of delayed neutrons	-3.29	-4.51
Six groups of delayed neutrons	-3.13	-4.36

Table 10: Critical values of coolant temperature coefficient of reactivity (α_c) for Static and Dynamic Bifurcations for the LMFBRs listed in Table 1.
(Core + Secondary Heat Exchanger using six groups of delayed neutrons)

Reactor	Critical values of α_c K^{-1}	
	α_c*(Static)	α_c*(Dynamic)
SUPER PHENIX	3.09×10^{-5}	-4.36
BELOYARSK-3	3.01×10^{-5}	-4.44
BELOYARSK-4	3.01×10^{-5}	-3.13
DFR	2.02×10^{-5}	-1.61
EBR-2	1.09×10^{-5}	-0.836
JOYO	4.37×10^{-5}	-2.78
KARLSRUHE	3.87×10^{-5}	-12.0
MANGYSHLASKI	2.78×10^{-5}	-1.07
MONJU	4.02×10^{-5}	-7.44
PHENIX	3.54×10^{-5}	-6.61
FBTR	3.01×10^{-5}	-2.46

4.3 Simultaneous variation of Parameters

As we have seen above, in each of the reactors studied, bifurcation occurs for possibly unrealistic values if parameters other than α_c are considered as constant . In this section, we vary other dimensionless parameters in certain ranges, with a view to find those sets of parameters for which bifurcations may occur for values of α_c more likely to occur in practice.

For this purpose the values attained by the dimensionless parameters for the SUPER-PHENIX reactor are treated as reference values and denoted by the subscript R. These are reproduced in Table 11 along with the ranges explored for each parameter. Ranges are selected with the help of Table 4, with a view to allow for the worst-case combination. The actual ranges tried, as given in Table 11, are broader than those strictly suggested in Table 4.

The worst case combinations of parameters are found using random trials. The results are shown in Table 12, for both static and Hopf bifurcations, together with the corresponding values of α_c^* (with and without secondary heat exchanger) using the expressions for the dimensionless parameters $a_f, b, c, \theta, p, r, \Theta$ given in chapter 2, the following ***physical interpretation*** may be given: both types of bifurcation are favored by

- A small magnitude of α_f
- A larger value of Λ and a small value of β
- A larger value of fuel to coolant heat capacity ratio
- Operating at larger power P
- A higher operating fuel temperature
- A lower heat capacity on the secondary side of the heat exchanger

Since most of the physical parameters enter into more than one dimensioless variables the above observations emphasize only the dominant effects.

Table 11 : Ranges of Parameter Ratios allowed for the worst case LMFBR

Reference Value†		Parameter Ratio	Range	
			Lower Limit	Upper Limit
a_{fR}	-1.045	a_f / a_{fR}	2.5	0.25
b_R	2×10^{-6}	b / b_R	0.1	10.0
c_R	0.652	c / c_R	0.4	3.0
θ_R	0.081	θ / θ_R	0.5	3.0
p_R	0.000019	p / p_R	0.01	10.0
r_R	0.000029	r / p	0.2	5.0
Θ_R	0.667	Θ / Θ_R	0.75	1.5

† Reference Values are for SUPER PHENIX as given in Table 2 and 4 and are here denoted by a subscript R

Table 12: Values of the Parameter Ratios for the worst case LMFBR for Static and Dynamic Bifurcations within the limits given in Table 11

Parameter Ratios	Worst case for	
	Static Bifurcation	Dynamic Bifurcation
a_f / a_{fR}	0.25	0.25
b / b_R	10.0	10.0
c / c_R	3.0	3.0
θ / θ_R	0.5	0.5
p / p_R	10.0	10.0
r / r_R	5.0	5.0
Θ / Θ_R	0.75	1.5
α_c^* (Without HE)	$+1.22\times10^{-5}K^{-1}$	$-2.6392\times10^{-1}K^{-1}$
α_c^* (With HE)	$+7.42\times10^{-6}K^{-1}$	$-3.8924\ K^{-1}$

It is, however, to be noted again, that even in the worst case situation, bifurcation values are impractical, except when the sodium temperature coefficient of reactivity may become positive.

4.4 Trajectories, Bifurcation Diagrams and Phase Portraits

As we have pointed above, an LMFBR dynamical system is unlikely to experience a bifurcation with the actual value of the parameters. In this section, we present numerically simulated trajectories/orbits and the bifurcation diagram for the worst case. Furthermore, as has been mentioned in Section 3.3, the static bifurcation is possible only when higher-order feedback effects are present. In the figures that follow, these effects are included for the transcritical bifurcation. In the case of Hopf bifurcation, we have ignored the higher-order feedback effects.

Figures 5 to 7 shows the time response for the dimensionless power $\wp$, dimensionless fuel temperatute $\Im_f$, and dimensionless coolant temperature $\Im_c$ subsequent to transcritical bifurcation. The parameter values for which these figures are plotted are shown on the figures. It can be seen that while the behavior of the linear system, or the system with linear feedback, is divergent, as expected, the behavior becomes bounded, as soon as any of the higher-order feedback effect is included. The presence of the new equilibrium point is indicated by the asymptotic approach for the same in Figures 5 to 7. The actual values at the new equilibrium point depend on how far the parameter α_c is from the bifurcation point. This is shown in Figure 8 to 10,
where

$$\text{Epsilon} \equiv \varepsilon \equiv \frac{\alpha_c - \alpha_c^*}{\alpha_c^*}.$$

The exchange of stability between the operating point and the new fixed point at the bifurcation is also clearly visible in these figures. The solid curves represent the stability while the dashed curves represent unstable condition.

It should however be mentioned that the new equilibrium point is only locally stable(in accordance with the local bifurcation theory). Thus all disturbed situations from the original operating point need not be in the basin of attraction of the new fixed point. The behavior shown in Figures 5 to 7 is valid only for those disturbances which are in the basin of attraction of the new equilibrium point. For other disturbances, the reactor behavior will remain divergent.

Figures 11 to 15 show the behavior subsequent to Hopf bifurcation in an LMFBR dynamical system using one and six groups of delayed neutrons, in the worst case. As has already been mentioned, the value of the parameter for which this behavior occurs appears to be extremely impractical. These figures, however, confirm the predictions of the theory described in Chapter 3. It may also be noted, that even this unlikely situation while the neutron flux may show large peaks, their effect on fuel and coolant temperature is limited (of the order of 20% to 30%).

The stability of the limit cycles represented in Figures 11 to 15 is further confirmed by the calculation of *stability parameter*, a(0), (3.2) and the characteristic multipliers shown in Table 13 . We mention here that as a(0)>0 , the situation similar to that shown in Figure 4c occurs in these models. In view of the unphysical nature of α_c^*, we will not consider the unstable limit cycles in the vicinity of the bifurcation point. These and their associated effects have been investigated by Manmohan (1996) in great detail.

4.5 Critical Values for the Control Parameters

As given in section 2.9, there are four control parameters K_p, t_p, K_c, and t_c. Table 14 gives the critical values α_c^*, for different values of K_p and t_p as compared to the situation without control ($K_p = 0$, $t_p = 0$). It can be seen that the bifurcation becomes all the more unlikely for all values of $K_p < 0$, the only situation that can occur in practice.

Table 15 shows the critical values of K_c for different values of t_c. It can be seen that K_c^* is of the order of (- 10^2 to -10^3). This, for the values of T_{co}, T_{io}, and β given in Tables 1 and 2, a control reactivity feedback of the order of -100 to -1000 $ per degree rise in sodium temperature. A practical value for the same is likely to be of the order of -10^{-1} to -10^{-2} $ per degree rise in the coolant temperature. Thus it can be concluded that the control system is unlikely to introduce any kind of bifurcation in the system.

Table 13: The stability parameter a and the characteristic (Floquet) multiplier for the LMFBR core limit cycle(worst case)

Parameter	One Group	Six Groups
Stability Parameter , a(0)	6.421×10^{-3}	6.426×10^{-3}
Floquet Multipliers ($\varepsilon = 0.005$)	0.999	----------
	0.235×10^{-1}	----------
	0.512×10^{-3}	----------

Table 14 : Critical values of the coolant temperature coefficient of reactivity (α_c) for different values of K_p and t_p for the reference reactor (SUPER PHENIX) Core + HE using six groups of delayed neutrons

K_p	t_p (s)	Critical values, α_c^*, K^{-1}	
		Static Bifurcation	Dynamic Bifurcation
0.0	-------	3.09×10^{-5}	-4.36
-0.1	0.0	8.31×10^{-4}	-3.7×10^{3}
	0.01	2.96×10^{-2}	-4.126
	0.1	0.288	-3.64
-1.0	0.0	8.03×10^{-3}	-3.48×10^{5}
	0.01	2.96×10^{-1}	-3.99×10^{1}
-10.0	0.0	8.00×10^{-2}	----------

Table 15: Critical values of the control parameter K_c (K_p=0, t_p=0) for Hopf bifurcation for Reference LMFBR (SUPER PHENIX).

t_c (s)	K_c^* (dimensionless)
0	-2.18×10^{2}
1.0×10^{-5}	-3.35×10^{2}
2.0×10^{-5}	-7.26×10^{2}
2.5×10^{-5}	-1.74×10^{3}

CENTRAL LIBRARY
I. I. T., KANPUR
Acc. No. A 126236

4.6 Conclusions and Observations

Based on the analytical and numerical results presented in this work, the following conclusions can be drawn :

- Models based on effective lifetime and prompt-jump approximations do not yield correct critical values. While these models may be quite useful in linear analysis, these should not be used for bifurcation studies.

- In lumped parameter dynamical systems including the core and the secondary heat exchanger, based on one and six groups of delayed neutrons, Hopf bifurcation is ruled out for physically realistic values of the parameters. This remains true for all (negative) gains in the proportional controllers, and any time constants associated with the differential controllers.
- Static bifurcation can occur only if the higher order feedback coefficients are present, of the three types of static bifurcation, saddle-node, pitch-fork and transcritical bifurcations it is shown in the present work that in the models considered only transcritical bifurcation can occur. However, this can occur only for *positive* values of coolant temperature coefficient of reactivity (α_c) of the order of 10^{-5} K^{-1}. For most LMFBRs, the values of α_c, while of the same order of magnitude, is likely to be negative.
- It is noted in the present work that subsequent to transcritical bifurcation, the new equilibrium point is only locally stable and may not be an attractor for all disturbances from the normal operating conditions. Thus there remain disturbances of the operating condition from which the reactor will show unstable divergent behavior in spite of the presence of higher order feedbacks

Some of the ***limitations*** of the present work and a few ***observations*** regarding future work in this area are given below:

- We have used lumped parameter models in the present work. Inclusion of the space variables in the models can modify / change the above conclusion. This should be included in future studies.
- In the present work, the control reactivity, whether based on change in reactor power or based on change in the coolant temperature, is assumed to act instantly. In future studies, appropriate governing equations for the control reactivity insertion should be included.
- We have ignored the transport times in the coolant pipes external to the reactor, leading the coolant from the reactor to the secondary heat exchanger. If the control signal based on coolant temperature is derived from measurement of the same across the secondary heat exchanger, the above mentioned transport times can play an important role. This should be included in future studies, together with any heat loss in the coolant pipes external to the reactor. The later effect will also modify the heat exchanger model. We may mention that the inclusion of the transport delay in nonlinear models necessitates a consideration of bifurcation theory of delay differential equation which has been outside the scope of the present work.
- In the present work, we have studied the local behavior in the vicinity of the bifurcation points. A global analysis may be attempted in future studies.
- Nonlinearities also effect the transient behavior of the reactor under normal operating parameter values. Their effect on the transients may have an important bearing on the optimal design of the controllers / control law. This can be a fruitful exercise to undertake in future.

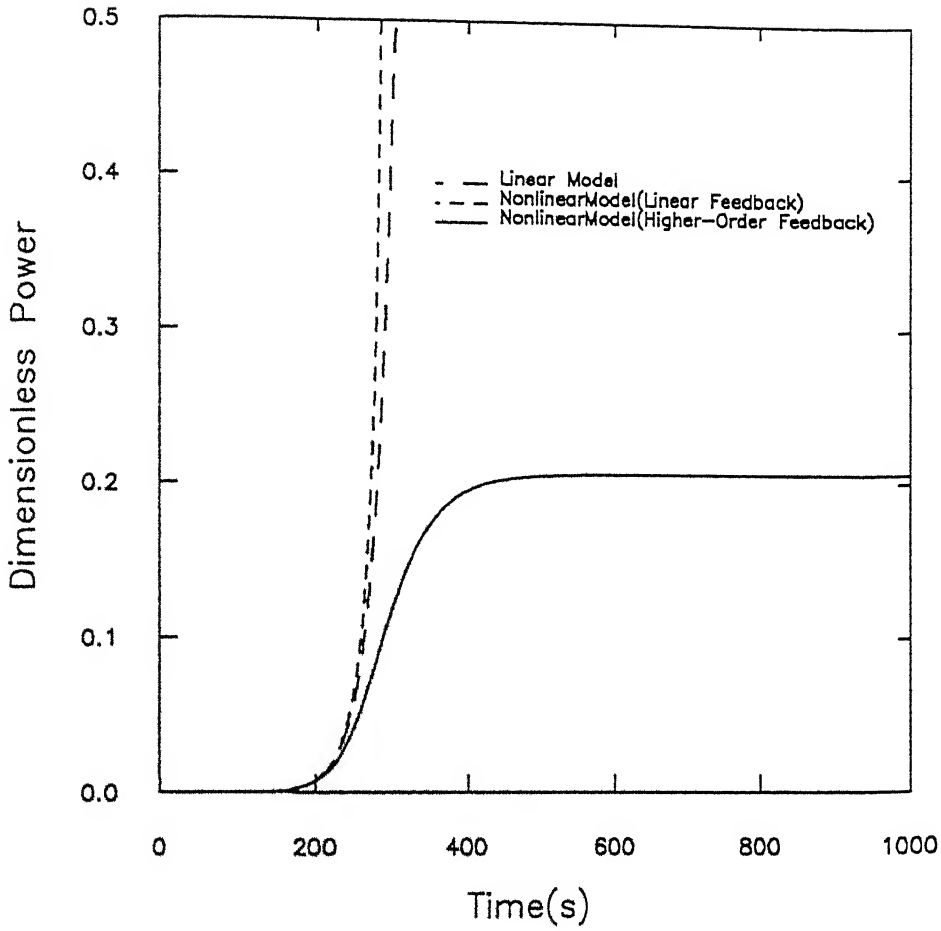

Figure 5: Time variation of dimensionless power $\wp$ subsequent to transcritical bifurcation in an LMFBR core (worst case) .

$$\left(\alpha_c = (1+\varepsilon)\alpha_c^*, \varepsilon = 1.5, \alpha_c^* = 1.22\times 10^{-5} K^{-1}, \frac{\alpha_F}{\alpha_f} = \frac{\alpha_C}{\alpha_c} = 0.01 K^{-1}\right)$$

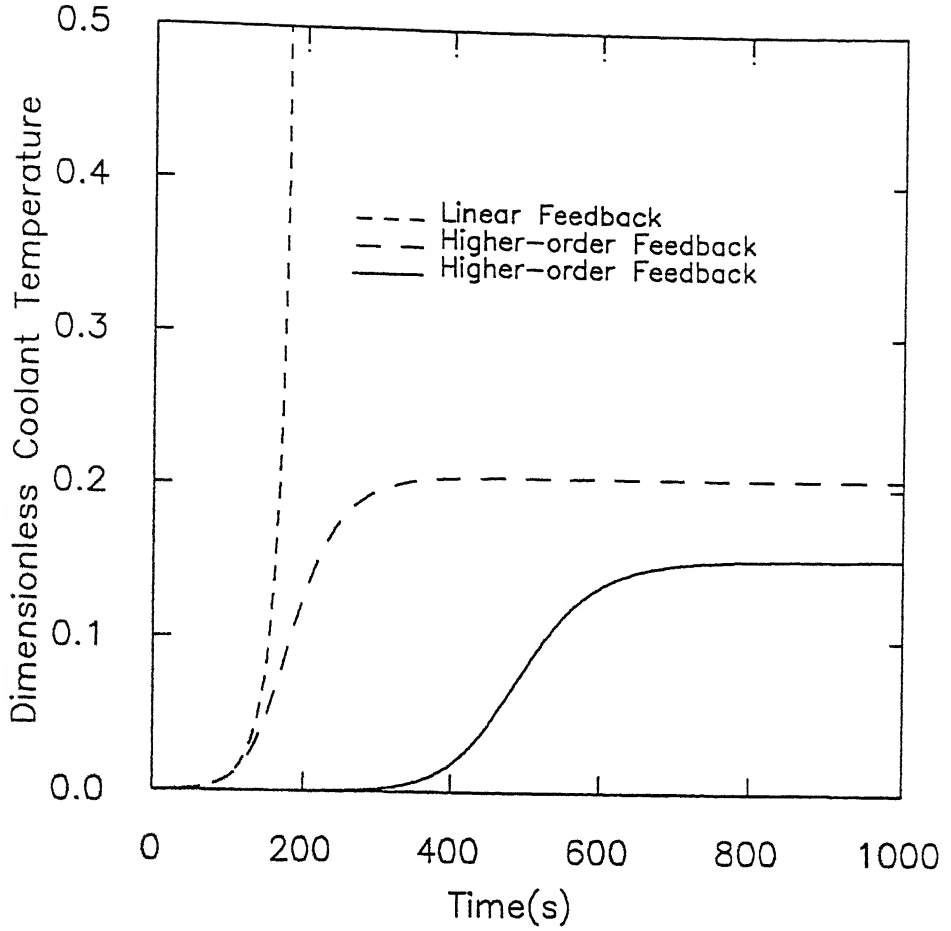

Figure 6 : Time variation of dimensionless coolant temperature $\Im_c$ subsequent to transcritical bifurcation in an LMFBR core (worst case).

$$- - \quad \left(\varepsilon = 1.5, \frac{\alpha_F}{\alpha_f} = \frac{\alpha_C}{\alpha_c} = 0.01K^{-1}\right)$$

$$— \quad \left(\varepsilon = 1.5, \frac{\alpha_F}{\alpha_f} = 0.1K^{-1}, \frac{\alpha_C}{\alpha_c} = 0.0\right)$$

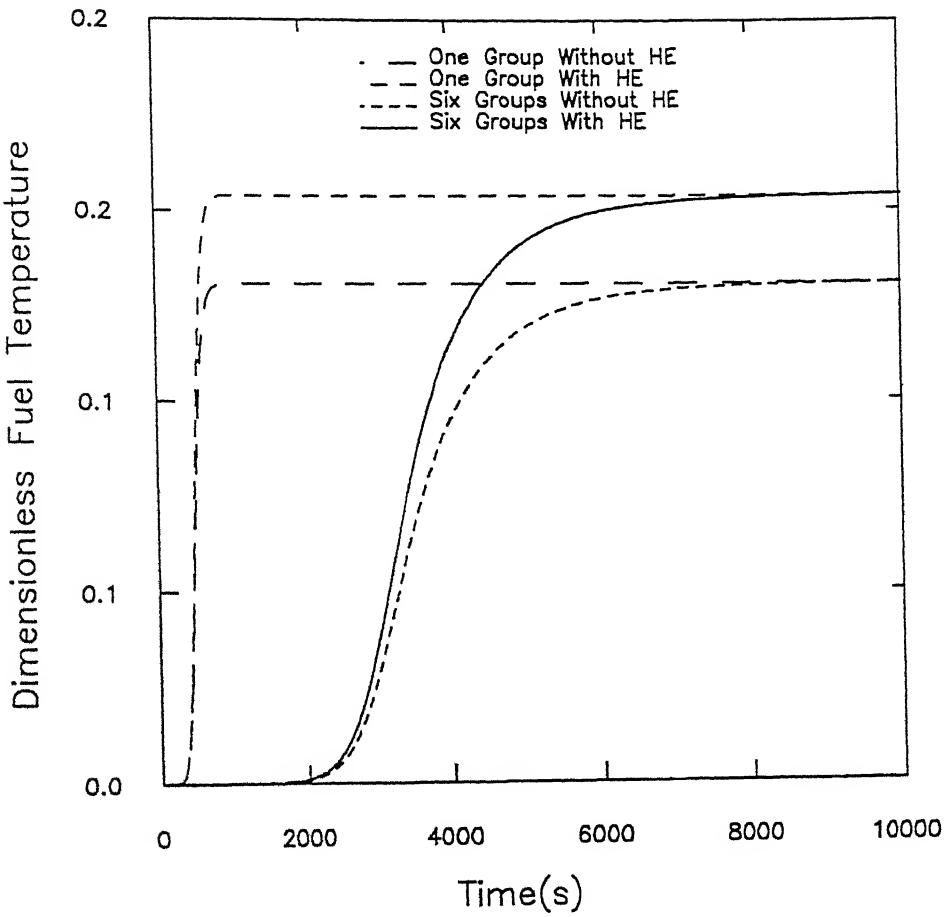

Figure 7: Effect of secondary heat exchanger and groups of delayed neutrons on time variation of dimensionless fuel temperature $\Im_f$ subsequent to transcritical temperature in a LMFBR core.

$$\left(\varepsilon = 1.0, \frac{\alpha_F}{\alpha_f} = \frac{\alpha_C}{\alpha_c} = 0.01K^{-1}\right)$$

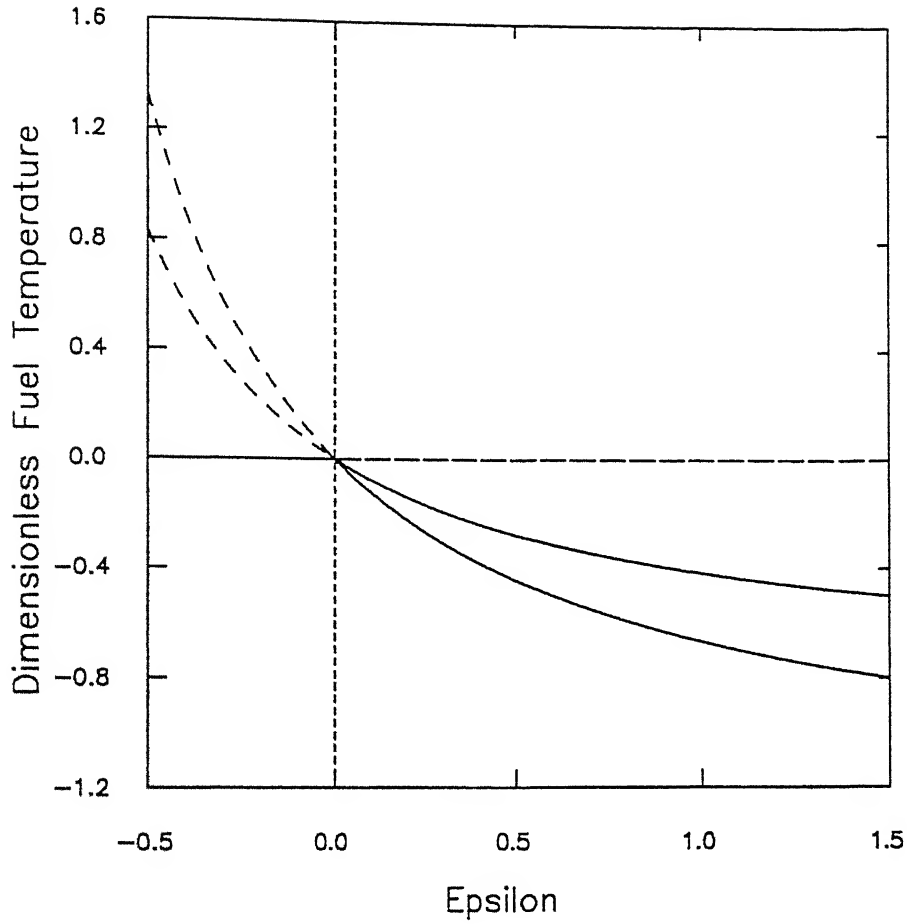

Figure 9 : Bifurcation diagram (with and without secondary heat exchanger) for transcritical bifurcation in the worst case LMFBR

$$\left(\frac{\alpha_F}{\alpha_f} = 0.0, \frac{\alpha_C}{\alpha_c} = 0.01K^{-1}\right)$$

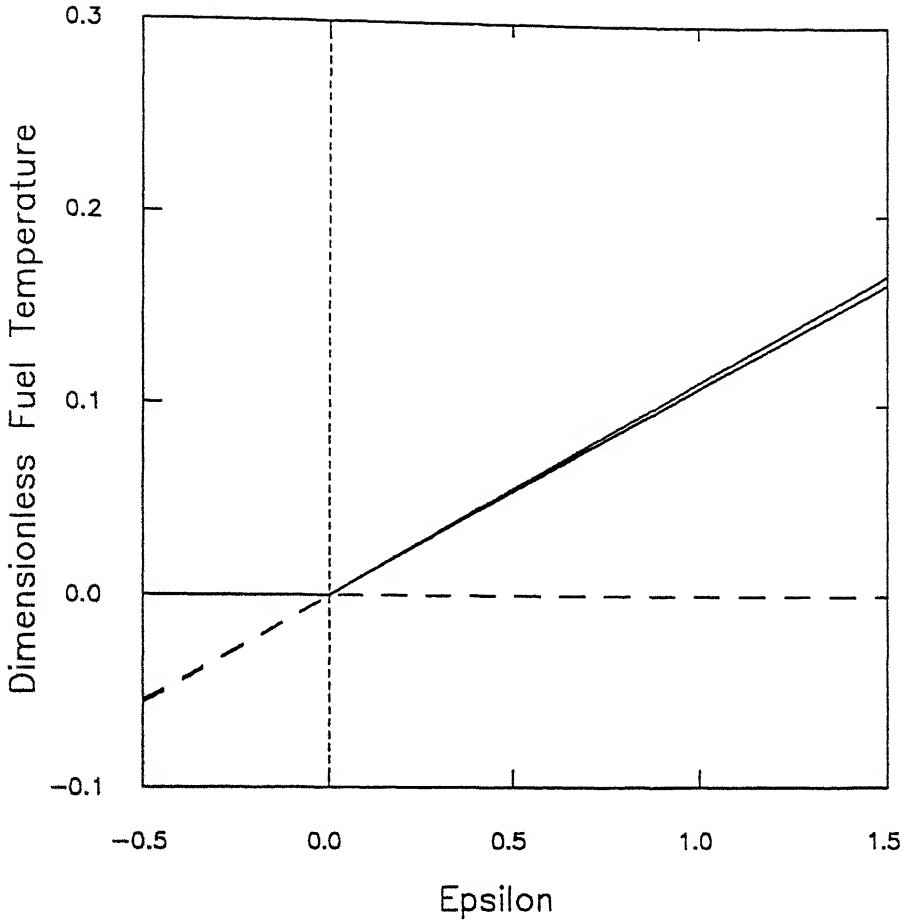

Figure 10 : Bifurcation diagram (with and without secondary heat exchanger) for transcritical bifurcation in the worst case LMFBR

$$\left(\frac{\alpha_F}{\alpha_f} = 0.01K^{-1}, \frac{\alpha_C}{\alpha_c} = 0.0\right)$$

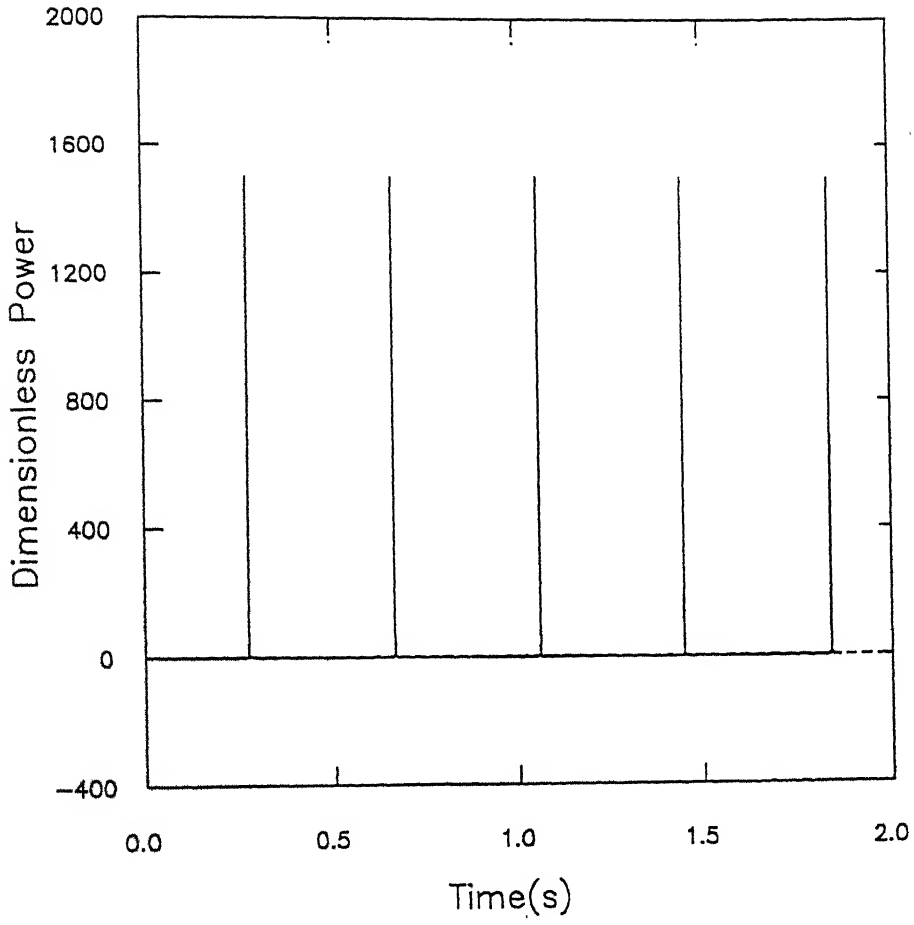

Figure 11 : Behavior of Dimensionless Power (neutron flux) versus time in LMFBR core (worst case) subsequent to Hopf bifurcation using one group of delayed neutrons ($\varepsilon = 0.01$)

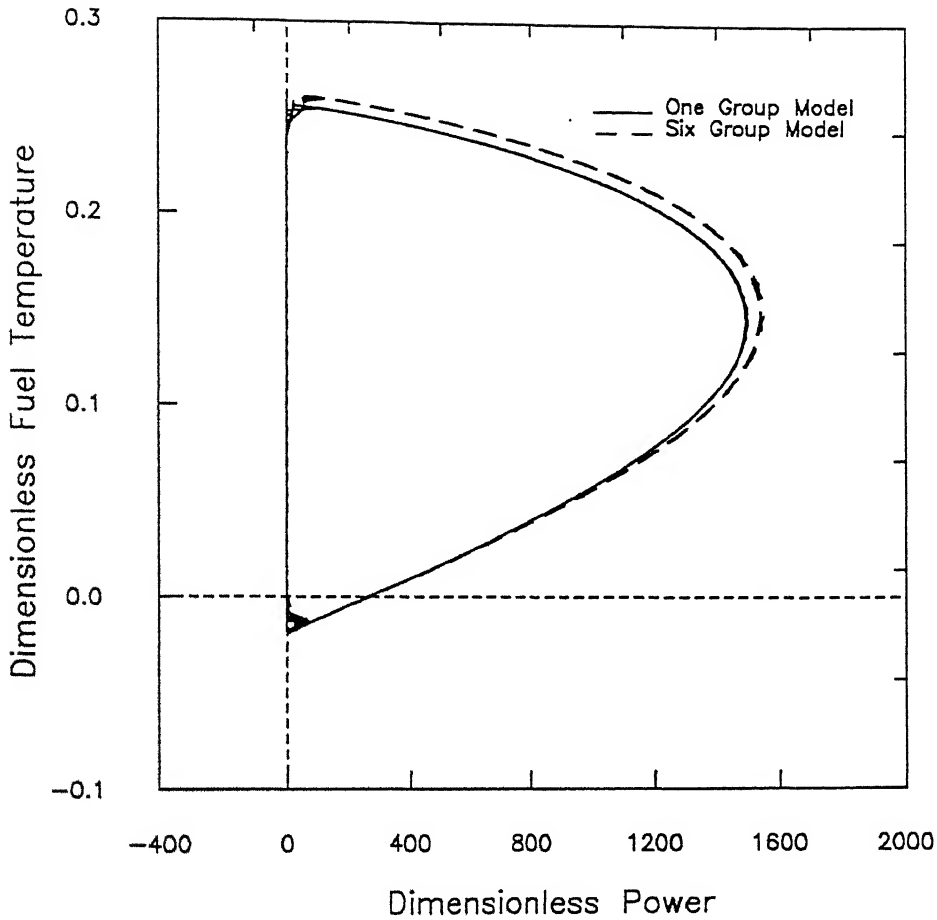

Figure 12 : Phase portrait of limit cycles in LMFBR models on $\wp - \Im_f$ plane (worst case) subsequent to Hopf bifurcation ($\varepsilon = 0.01$).

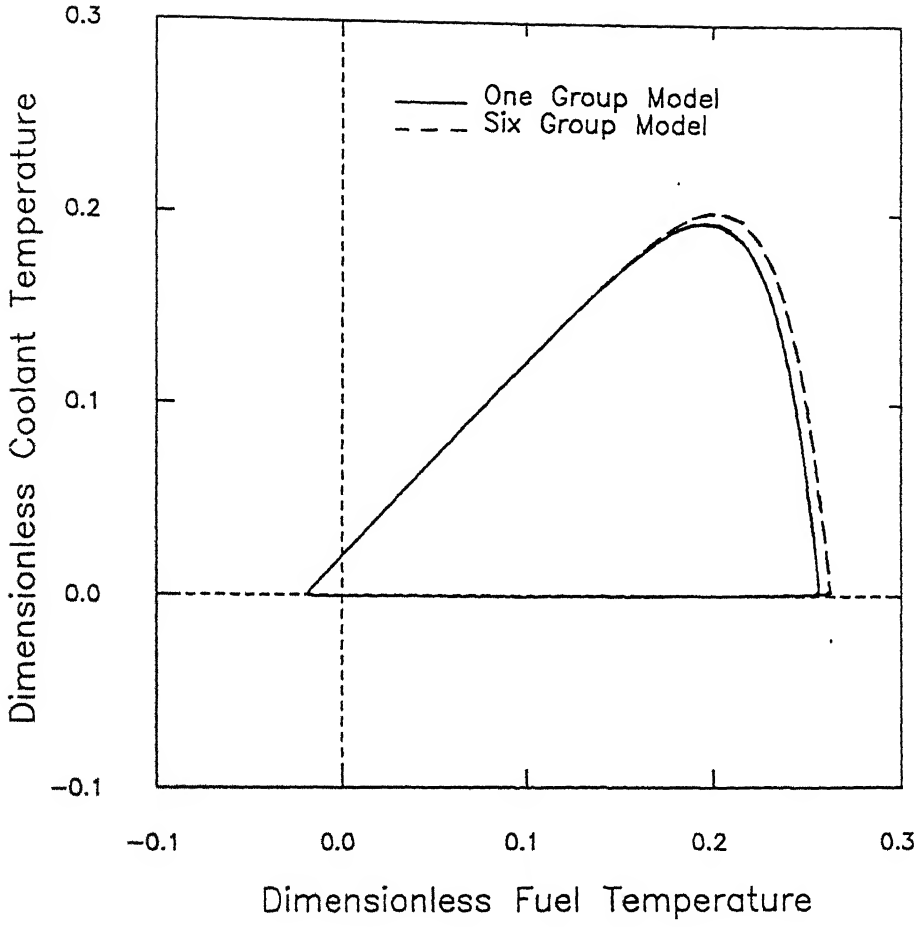

Figure 13 : Phase portrait of limit cycles in LMFBR models on $\Im_f - \Im_c$ plane (worst case) subsequent to Hopf bifurcation ($\varepsilon = 0.01$)

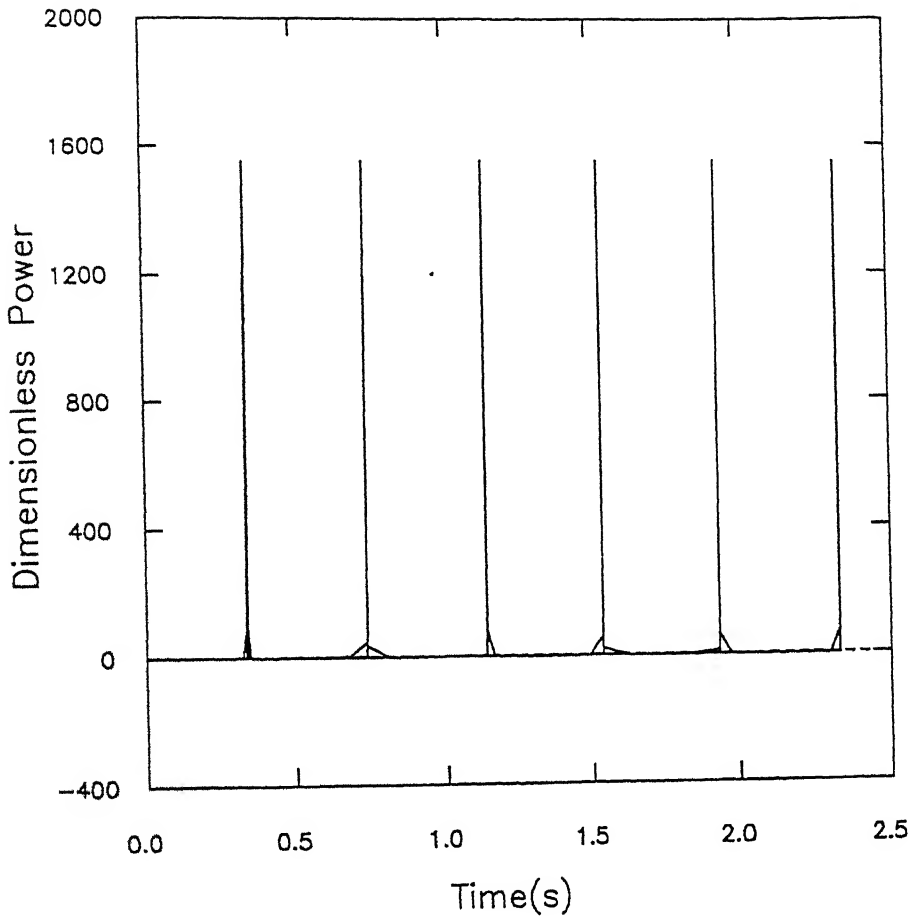

Figure 14 : Behavior of Dimensionless Power (neutron flux) versus time in LMFBR core (worst case) subsequent to Hopf bifurcation using six groups of delayed neutrons ($\varepsilon = 0.01$)

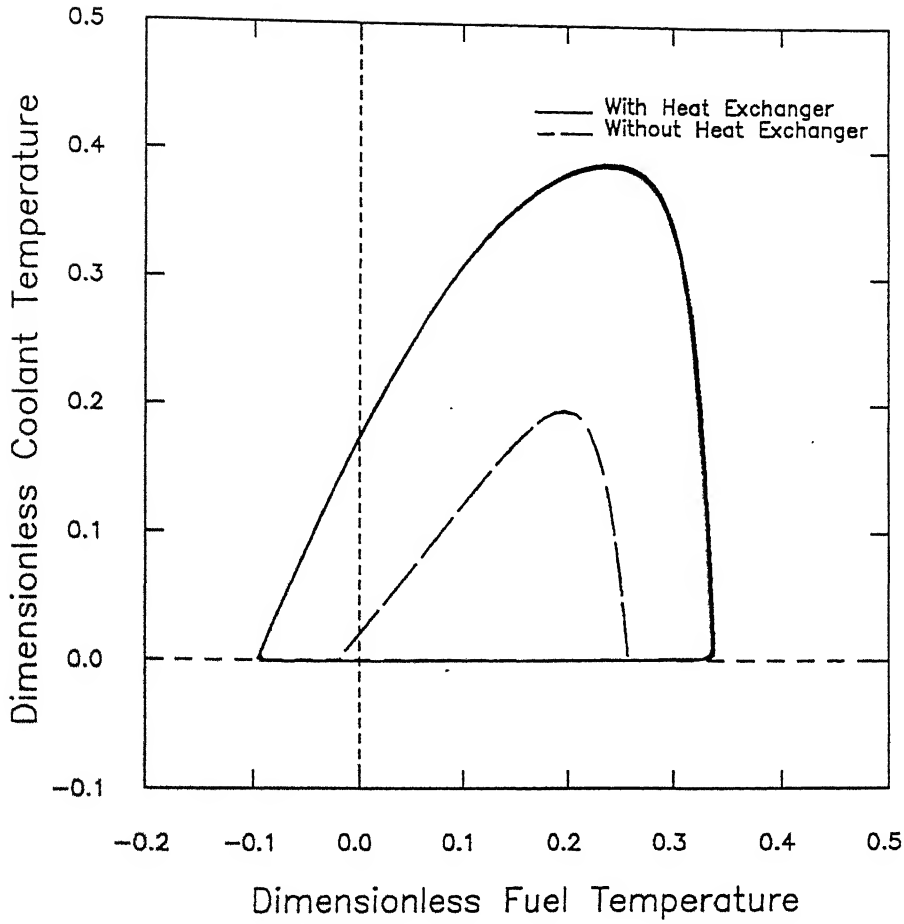

Figure 15 : Effect of secondary heat exchanger on the limit cycles in the worst case LMFBR subsequent to Hopf bifurcation ($\varepsilon = 0.01$)

References

Adebiyi, S. A. and Harms, A. A. (1989). On the topology of linear and nonlinear reactor kinetics. *Annals of Nuclear Energy*, **16**(11):605-609.

Adebiyi, S. A. and Harms, A. A. (1990). Behavioral geometrics of nonlinear reactor dynamics. *Journal of Nuclear Science and Technology*, 27(5):416-430.

Agrawal, A. K. , Guppy, J. G. , Madni, I. K. , Quan, V. , Weaver, W. L. , and Yang, J. W. (1977). Simulation of Transients in Liquid Metal Fast Breeder Reactor Systems. *Nuclear Science and Engineering*, **64**: 480-491.

Bergdhal, B. G., *et al.* (1989). BWR stability investigation at forsmark 1. *Annals of Nuclear Energy*, **16**(10):509-520.

Chernick, Jack (1951). The dependence of reactor kinetics on temperature. Technical report, Brookhaven National Laboratory, Upton, N.Y., U.S.A.

Constantine ,Tzanos P. (1987). Liquid Metal Fast Breeder Reactor Core Transient Modeling for Faster than Real Time-Analysis. *Journal of Nuclear Technology*, 77: 263-268.

Dorning, J. (1989). Is there a strange attractor in your reactor? *Transaction of the American Nuclear Society*, **60**:341-342.

Enginol, Turan B. (1985). On the asymptotic stability of nuclear reactors with arbitrary feedback. *Nuclear Science and Engineering,* **90**:231-235.

Guckenheimer, John and Holmes, Philip (1983). *Nonlinear Oscillations, Dynamical Systems, and Bifurcations of Vector Fields.* Springer-Verlag.

Hetrick, David L. (1965). A liapunov function in reactor dynamics. *Transactions of the American Nuclear Society*, **8**:477.

Hetrick, David L. (1971). *Dynamics of Nuclear Reactors.* University of Chicago Press.

Hsu, Chun (1968). A stability criterion for spatially dependent nonlinear reactor systems. *Transactions of the American Nuclear Society*, **11**:223.

Hsu, T. and Sha, W. T. (1969). Determination of stability domain of nonlinear reactor dynamics. *Transactions of the American Nuclear Society*, **12**:295.

Husseyin, Koncay (1986). *Multi Parameter Stability Theory and Its Applications: Bifurcations, Catastrophies,*...Clarendon Press.

Kalra, M. S. and Sriram, K. (1998). Impact of nonlinear reactivity interactions and power excursions on safe operation of nuclear reactors. Consolidated report (Phase 1 and 2), *Atomic Energy Regulatory Board*, India.

Karl Wirtz (1973). Lectures on Fast Reactors.

Kastenberg, William E. (1968). On the stability of a reactor with arbitrary feedback. *Transactions of the American Nuclear Society*, **11**:224.

Kubicek, M. and Marek, M. (1983). *Computational Methods in Bifurcation Theory and Dissipative Structures.* Springer-Verlag.

Lewins, J. (1978). *Nuclear Reactor Kinetics and Control.* Pergamon Press.

Manmohan, P. (1996). Nonlinear reactivity interactions in fission reactor dynamical systems. Ph.D. thesis, Indian Institute of Technology Kanpur.

Parker, T. S. and Chua, L. O. (1989). *Practical Numerical Algorithms for Chaotic Systems.* Sringer-Verlag.

Paul B. Bleiweis. (1975). Computational Models for the Study of Azimuthally Dependent Disassembly of Liquid Metal Fast Breeder Reactors. *Nuclear Science and Engineering*, **56**: 152-170.

Power Reactors (1983). Annual directory of data on the world's nuclear power reactors. *Supplement to Nuclear Engineering International, volume 28.*

Press, William H., et al. (1993). *Numerical Recipes in FORTRAN: The Art of Scientific Computing.* Cambridge University Press.

Robinson, Lawrence Baylor (1954). Concept of stability of nuclear reactors. *Journal of Applied Physics*, **25**:516-518.

Robinson, Lawrence Baylor (1955). Effect of delayed fission neutrons on reactor kinetics. *Journal of Applied Physics*, **26**:52-56.

Ruelle, David (1989). *Chaotic Evolution and Strange Attractors*. Cambridge University Press.

Samuel Glasstone. and Alexander Sesonske (1994). *Nuclear Reactor Engineering*. Chapman and Hall Inc.

Ward, Mary E. and Lee, John C. (1987a). Singular perturbation analysis of limit cycle behavior in nuclear-coupled density-wave oscillations. *Nuclear Science and Engineering*, **97**:190-202.

Ward, Mary E. and Lee, John C. (1987b). Singular perturbation analysis of relaxation oscillations in reactor systems. *Nuclear Science and Engineering*, **95**:47-59.

Weston , Stacey Jr M. (1972). An improved Reactivity Table Model for Liquid Metal Fast Breeder Reactor Dynamics. *Nuclear Science and Engineering*, **49**: 213-227.

Wiggins, Stephen (1989). *Introduction to Nonlinear Dynamical Systems and Chaos*. Springer-Verlag.

Vilim, R. B. Wei, T. Y. C. and Dunn, F. E. (1988). Generalized Control System Modeling for Liquid Metal Reactors. *Nuclear Science and Engineering*, **99**: 183-196.

World Nuclear Industry Handbook (1994). *Nuclear Engineering International*.

Yang, Chae Yong and Cho, Nam Zin (1992). Expansion methods for finding nonlinear stability domains of nuclear reactor models. *Anals of Nuclear Energy* , **19**(6):347-368.

Appendix A

Sample Calculation of C_f and C_c for Reference LMFBR SUPER PHENIX.

For this reference reactor SUPER PHENIX, we have, (Power Reactors (1983))

Estimation of C_f

Active core height, $H = 1.0m$

Active core diameter $D = 3.66m$

Fuel pellet diameter, $d = 7.14 \times 10^{-3} m$

Clad thickness, $t = .57 \times 10^{-3} m$

Fuel inventory, $m_f = 31.5 \times 10^3 kg$

Fuel density (U/Pu metal), $\rho_f = 19000 \text{ kg m}^{-3}$

Specific heat (U/Pu metal), $c_f = 0.17 \text{ KJ kg}^{-1} \text{ K}^{-1}$

$C_f = m_f c_f = 5.355 \text{ MJK}^{-1}$

Estimation of C_c

Core volume, $V = (\pi/4)D^2H = 10.62 \text{ m}^3$

Fuel volume , $V_{fuel} = m_f / \rho_f = 1.6 \text{ m}^3$

$V_{structure} / V_{fuel} = (V_{clad} / V_{fuel}) \times 1.2 = (t(d+t) / d^2) \times 1.2 = 0.414$

(20% additional structure volume over and above the clad volume allowed in the core.)

$V_{structure} / V = 0.16 \times 0.414 = 0.066$

$(V_{fuel} + V_{structure}) / V = 0.226$

$V_{coolant} / V = 0.774,$

$V_{coolant} = 8.21 m^3$

$\rho_{coolant}$ (Na) = 800 Kgm^{-3}

$m_{coolant} = \rho_c V_c = 800 \times 8.21 = 6576 Kg$

$C_c = m_c c_c = 7.91 MJK^{-1}$

Other Reactors

The core/fuel data for other reactors is given in Table A. For calculations in the present work , densities and specific heats are taken as follows

ρ (UO_2 / PuO_2) = 11000 kgm^{-3}

c (UO_2 / PuO_2) = 0.32 KJ kg^{-1} K^{-1}

ρ (UC / PuC) = 13630 kg m^{-3}

c (UO_2 / PuO_2) = 0.25 KJ $kg^{-1}K^{-1}$

Table A : Core fuel data for the representative LMFBRs

Reactor	Fuel Inventory (t)	Core Height (m)	Core Diameter (m)	Fuel Rod Diameter (m)	Clad thickness (m)
SUPER PHENIX	31.5	1.0	3.66	7.14×10^{-3}	0.57×10^{-3}
BELOYARSK-3	8.5	0.75	2.05	5.9×10^{-3}	0.4×10^{-3}
BELOYARSK-4	8.5	0.75	2.05	5.9×10^{-3}	0.4×10^{-3}
DFR	0.34	0.53	0.53	4.95×10^{-3}	0.5×10^{-3}
EBR-2	0.46	0.36	0.65	4.4×10^{-3}	0.3×10^{-3}
JOYO	0.25	0.55	0.73	4.6×10^{-3}	0.35×10^{-3}
KARLSRUHE	0.728	0.6	0.82	6.4×10^{-3}	0.5×10^{-3}
MANGYSHLASKI	1.22	1.0	1.58	5.9×10^{-3}	0.4×10^{-3}
MONJU	5.9	0.93	1.79	4.5×10^{-3}	0.47×10^{-3}
PHENIX	4.3	0.85	1.39	5.1×10^{-3}	0.45×10^{-3}
FBTR	0.19	0.32	0.43	3.65×10^{-3}	0.37×10^{-3}

126236

Date Slip 126236

This book is to be returned on the date last stamped.

NETP-1988-M-BAL-TRA